

**Editor Decision: Reconsider after minor revisions (Editor review)** (12 Mar 2016) by Willy Maenhaut  
Comments to the Author:

We thank for the thoughtful and detailed comments. Below we respond to the comments.

First, the Supplement is missing. There is a tar file with "supplement" in its name, but it does not contain the Supplement.

The supplement was added to Supplement section as pdf.

Furthermore, several alterations are still needed in the main text before this manuscript can be published in ACP. For the main text:

I wrote "References that are listed in parentheses within the text should be separated by a semicolon instead of by a comma". This was not always implemented; for example not on page 15, lines 19-20. Page 3, line 2: Replace "90 %" by "90%".

The separations by semicolon were done:

Page 2, lines 28, 29 and 32;

Page 3, lines 13, 26;

Page 10, line 6;

Page 15, lines 19-20.

Page 3, line 3 "90 %" replaced by "90%".

Page 6, line 24: Replace "Ångstrom" by "The Ångstrom".

Page 6, line 24: " Ångström " replaced by "The Ångström".

Page 13, line 10: Replace "previous years" by "that in previous years".

Page 13, line 9-10: "previous years" replaced by "that in previous years".

Page 13, line 20: Replace "west part of Lithuania are moderate" by "the western part of Lithuania are a moderate".

Page 13, line 20-21: "west part of Lithuania are moderate" replaced by "the western part of Lithuania are a moderate".

Page 14, line 31: Replace "Observed NPF" by "The observed NPF events".

Page 14, line 31: "Observed NPF" replaced by "The observed NPF events".

Page 15, line 2: Replace "The total particle" by "A total particle".

Page 15, line 2: "The total particle" replaced by "A total particle".

Page 16, line 21: Replace "respectively). (Ulevicius" by "respectively) (Ulevicius".

Page 16, line 22: "respectively). (Ulevicius" replaced by "respectively) (Ulevicius".

Page 17, line 10: Replace "0.3 to 1.1" by "0.3 to 1.1  $\mu\text{g m}^{-3}$ ".

Page 17, line 11: "0.3 to 1.1" replaced by "0.3 to 1.1  $\mu\text{g m}^{-3}$ " and "1.6  $\mu\text{gm}^{-3}$ " by "1.6  $\mu\text{g m}^{-3}$ ".

Pages 19-31, Reference list: I wrote: "For references with at least 3 authors there should be ", and" before the last author; note that for references with only 2 authors there should be NO comma before the "and" before the last author". This was not always implemented; for example not on page 28, line 13, and on page 28, line 27. Furthermore, the "and" was not always properly preceded by a comma when needed; e.g., not on page 28, lines 20 and 25.

References was corrected:

Page 22, line 13, 27

Page 23, lines 8-12

Page 24, lines 19-21

Page 26, line 19

Page 27, lines 19, 28  
 Page 28, lines 1, 14, 16, 23, 27-30  
 Page 29, lines 1, 14  
 Page 31, line 11

Page 28, line 11: Replace "Atm. Env." by "Atmos. Environ.".

Page 28, line 14: "Atm. Env." replaced by "Atmos. Environ.".

Page 33, Table 1: The footnotes "2" and "3" within the table do not correspond with the explanations in footnotes "2" and "3" under the table. Furthermore, it is still not clear what the numbers in parentheses for the "Tree cover" and "Herbaceous cover" (and incidentally also for "Water bodies") indicate.

Footnotes was corrected. The numbers in parentheses mean GLC2000 classes ID. It was explained after the table.

Page 33, footnote 1 under Table 1: Replace "100 %" by "100%" and "50 %" by "50%".  
 Page 41, Table 3: I wrote "several numeric data in the table have too many significant figures; three would suffice". Nothing was done here; the numeric data should have less significant figures (digits).

Page 33, footnote 1 under Table 1: "100 %" replaced by "100%" and "50 %" replaced by "50%".

The Table 3 was corrected. The number of significant figures in the values was limited to one (to maintain the balance =100.0).

Table 3. Average percentage contributions of different sources

Relative contributions [%] to TC	POCf	POCnf	SOCf	SOCnf	ECf	ECnf	TC to PM1
2014.03.05	5.1	43.2	6.7	22.5	9.7	12.8	28.4
2014.03.07	6.2	43.6	5.7	19.1	6.6	18.8	37.6
2014.03.08	7.7	26.3	13.4	18.6	12.6	21.4	24.8
2014.03.09	4.5	41.3	4.4	13.1	12.5	24.2	51.3
2014.03.10	6.8	43.0	5.9	14.8	7.2	22.3	43.9
Relative contributions [%] to OC	POCf	POCnf	SOCf	SOCnf			
2014.03.05	6.6	55.8	8.6	29.0			
2014.03.07	8.4	58.4	7.6	25.6			
2014.03.08	11.7	39.8	20.2	28.3			
2014.03.09	7.2	65.2	6.9	20.7			
2014.03.10	9.6	61.0	8.4	21.0			

1 **Fossil and non-fossil source contributions to atmospheric**  
2 **carbonaceous aerosols during extreme spring grassland**  
3 **fires in Eastern Europe**

4

5 **V. Ulevicius<sup>1</sup>, S. Byčenkienė<sup>1</sup>, C. Bozzetti<sup>2</sup>, A. Vlachou<sup>2</sup>, K. Plauškaitė<sup>1</sup>, G.**  
6 **Mordas<sup>1</sup>, V. Dudoitis<sup>1</sup>, G. Abbaszade<sup>3</sup>, V. Remeikis<sup>1</sup>, A. Garbaras<sup>1</sup>, A. Masalaite<sup>1</sup>,**  
7 **J. Blees<sup>2</sup>, R. Fröhlich<sup>2</sup>, K. R. Dällenbach<sup>2</sup>, F. Canonaco<sup>2</sup>, J. G. Slowik<sup>2</sup>, J.**  
8 **Dommen<sup>2</sup>, R. Zimmermann<sup>3,4</sup>, J. Schnelle-Kreis<sup>3</sup>, G. A. Salazar<sup>5</sup>, K. Agrios<sup>5,6</sup>, S.**  
9 **Szidat<sup>5</sup>, I. El Haddad<sup>2</sup> and A. S. H. Prévôt<sup>2</sup>**

10 [1] Department of Environmental Research, SRI Center for Physical Sciences and  
11 Technology, Vilnius, Lithuania

12 [2] Laboratory of Atmospheric Chemistry, Paul Scherrer Institute (PSI), 5232 Villigen,  
13 Switzerland

14 [3] Helmholtz Zentrum München, German Research Center for Environmental Health  
15 (GmbH), Joint Mass Spectrometry Centre, Cooperation Group Comprehensive Molecular  
16 Analytics and Helmholtz Virtual Institute of Complex Molecular Systems in Environmental  
17 Health – Aerosol and Health (HICE), 85764 Neuherberg, Germany

18 [4] Analytical Chemistry & Joint Mass Spectrometry Centre, Institute of Chemistry,  
19 University of Rostock, Dr.-Lorenz-Weg 1, D-18051 Rostock /Germany

20 [5] Department of Chemistry and Biochemistry & Oeschger Centre for Climate Change  
21 Research, University of Bern, 3012 Bern, Switzerland

22 [6] Laboratory of Radiochemistry and Environmental Chemistry, PSI, 5232 Villigen,  
23 Switzerland

24 Correspondence to: V. Ulevicius and A. S. H. Prévôt ([ulevicv@ktl.mii.lt](mailto:ulevicv@ktl.mii.lt),  
25 [andre.prevot@psi.ch](mailto:andre.prevot@psi.ch))

26

27

28

1 **Abstract**

2 In early spring the Baltic region is frequently affected by high pollution events due to  
3 biomass burning in that area. Here we present a comprehensive study to investigate the  
4 impact of biomass/grass burning (BB) on the evolution and composition of aerosol in Preila,  
5 Lithuania, during springtime open fires. Non-refractory submicron particulate matter (NR-  
6 PM<sub>1</sub>) was measured by an Aerodyne aerosol chemical speciation monitor (ACSM) and a  
7 source apportionment with the multilinear engine (ME-2) running the positive matrix  
8 factorization (PMF) model was applied to the organic aerosol fraction to investigate the  
9 impact of biomass/grass burning. Satellite observations over regions of biomass burning  
10 activity supported the results and identification of air mass transport to the area of  
11 investigation. Sharp increases in biomass burning tracers, such as levoglucosan up to 683 ng  
12 m<sup>-3</sup> and black carbon (BC) up to 17 µg m<sup>-3</sup> were observed during this period. A further  
13 separation between fossil and non-fossil primary and secondary contributions was obtained by  
14 coupling ACSM PMF results and radiocarbon (<sup>14</sup>C) measurements of the elemental (EC) and  
15 organic (OC) carbon fractions. Non-fossil organic carbon (OC<sub>nf</sub>) was the dominant fraction of  
16 PM<sub>1</sub>, with the primary (POC<sub>nf</sub>) and secondary (SOC<sub>nf</sub>) fractions contributing 26-44% and 13-  
17 23% to the total carbon (TC), respectively. 5–8% of the TC had a primary fossil origin  
18 (POC<sub>f</sub>), whereas the contribution of fossil secondary organic carbon (SOC<sub>f</sub>) was 4–13%. Non-  
19 fossil EC (EC<sub>nf</sub>) and fossil EC (EC<sub>f</sub>) ranged from 13–24% and 7–13%, respectively. Isotope  
20 ratios of stable carbon and nitrogen isotopes were used to distinguish aerosol particles  
21 associated with solid and liquid fossil fuel burning.

22

23 **1 Introduction**

24 On a global scale wood or grass burning is a major source of organic aerosol (Crutzen et al.,  
25 1979; Levine, 1996). Approximately 90% of vegetation burning is caused by human-induced  
26 fires (Baldini et al., 2002) and only a minor fraction derives from natural processes such as  
27 lightning. The composition of biomass smoke depends on the type of wood, combustion  
28 conditions (flaming versus smoldering), and ambient weather conditions (Weimer et al., 2008;  
29 Grieshop et al., 2009; Hawkins and Russell, 2010; Akagi et al., 2012). Fine particles emitted  
30 from biomass burning include directly emitted primary particles (POA) and secondary  
31 organic aerosols (SOA), formed in the atmosphere as the plume ages through photochemical  
32 processes driven by sunlight (Capes et al., 2008; Heringa et al., 2011).

Deleted: ,

Deleted: ,

Deleted:

Deleted: and

Deleted: ,

1 Many studies have revealed that organic matter (OM) is the largest fraction of ambient fine  
2 particles, typically comprising 20–90% of the submicron particulate mass (Jimenez et al.,  
3 2009). Factor analysis of aerosol mass spectra from the Aerodyne aerosol mass spectrometer  
4 enables the deconvolution of OM into different factors based on their mass spectral  
5 fingerprints (Lanz et al., 2007; Aiken et al., 2009; Ulbrich et al., 2009). Such results provided  
6 valuable insights into the source and transformation processes of organic aerosols (OA) in the  
7 atmosphere (Lanz et al., 2010; Ng et al., 2011; Hildebrandt et al., 2011; Canonaco et al. 2013;  
8 Bougiatioti et al., 2014; Huang et al., 2014).

Deleted:

9 The main type of biomass burning in Lithuania and surrounding countries in early spring  
10 during the last years is illegal [grass burning](#) for land clearing (Ulevicius et al., 2010b;  
11 Byčenkienė et al. 2013). The north-east European countries are considered to influence  
12 significantly the microphysical, chemical and optical properties of the aerosol in the Baltic  
13 Sea region (Kikas et al., 2008; Zawadzka et al., 2013; Mann et al., 2014; [Beddows et al.](#),  
14 2014). Long-term measurements of carbonaceous aerosols performed in this area by Ulevicius  
15 et al. (2010a, 2010b) and Byčenkienė et al. (2011, 2013) reported a yearly occurrence of high  
16 biomass burning organic aerosol (BBOA) levels during March–April related to regional  
17 transport from the Kaliningrad region, Ukraine and the southwestern part of Russia  
18 surrounding the Black Sea, but information on the nature and chemical composition of the  
19 biomass burning aerosol in Lithuania is still limited. There has been no systematic  
20 investigation of the impact of biomass burning on ambient organic aerosol levels in this  
21 region, and a quantitative estimate is needed to understand the possible impacts of BBOA on  
22 air quality in the south-eastern Baltic Sea region.

Deleted: .

23 In many studies levoglucosan was used to assess the contribution of biomass-burning smoke  
24 to the aerosol mass concentrations (Puxbaum et al., 2007). A number of source emission  
25 studies reported that levoglucosan is not a useful tracer after long-range transport due to its  
26 transformation (Hoffmann et al., 2010; [Hennigan et al.](#), 2010; Mochida et al., 2010). In  
27 contrast to levoglucosan, determination of radiocarbon ( $^{14}\text{C}$ ) offers a unique possibility for  
28 source apportionment of carbonaceous aerosol particles, as it unambiguously distinguishes  
29 fossil from non-fossil emissions (e.g., Currie, 2000; Ceburnis et al., 2011).

Deleted: .

30 For this study, in the framework of the Lithuanian-Swiss Cooperation Programme joint  
31 research project (AEROLIT), an aerosol chemical speciation monitor (ACSM) was deployed  
32 in a background area of the South Baltic Sea to measure airborne submicron particles for one  
33 month during a period of frequent grass burning pollution. The main findings include

1 investigation of OA components (Sects. 3.1–3.2), molecular markers (Sect. 3.2), source  
2 apportionment of elemental and organic carbon (EC and OC) using  $^{14}\text{C}$  data and positive  
3 matrix factorization (PMF) of the ACSM organic mass spectra (Sect. 3.3).

## 4 **2 Methods**

### 5 **2.1. Site description and filter sampling**

6 Continuous air monitoring and time integrated particulate matter sampling were carried out in  
7 March 2014 in Preila, Lithuania (55° 55' N, 21° 04' E 5 m a.s.l.) (Fig. 1). Preila is a  
8 representative coastal background site, an ideal location for studying the long-range transport  
9 of air pollutants in the South-eastern Baltic region due to the absence of significant local  
10 sources (Fig. 1, Table 1). It served as a “super site” for the EUSAAR-EU-funded (Integrated  
11 Infrastructures Initiatives) project. During the measurement period, strong biomass burning  
12 activities were observed on 9–10 March 2014. A high-volume sampler (Digital model  
13 Aerosol Sampler DHA-80, 500 L min<sup>-1</sup>) was used to collect PM<sub>1</sub> aerosol particles onto 150  
14 mm diameter Pallflex quartz fibre filters (pre-baked for 24 h at 550 °C) over a 24-hour  
15 sampling period. Filters were stored in a freezer (at -20 °C) immediately after sampling.

### 16 **2.2. Instrumentation**

#### 17 **2.2.1. Aerosol Chemical Speciation Monitor and data analysis**

18 An ACSM (Aerodyne Research, Inc., Billerica, MA, USA) was deployed to measure  
19 PM<sub>1</sub> components in Preila (Fig. 1, Sect. 2.1). A PM<sub>10</sub> impactor-type inlet was utilized to  
20 remove coarse particles from the sample stream. The sampling air (1.1 L min<sup>-1</sup>) passed  
21 through a vertical 2.5 m long stainless steel tube with a 6 mm i.d. and a Nafion dryer (MD-  
22 110-12S-4, PermaPure LLC, Toms River, NJ, USA) before reaching the device. Aerosol  
23 particle diffusion losses in the sampling line were less than 4.0% for particles from 40 nm to 1  
24 μm according to Gormley and Kennedy (Baron and Willike, 2001) and the relative humidity  
25 lower than 50% (by SATO model SK-L200TH). Thus, the used sampling line and ambient  
26 relative humidity did not affect aerosol mass concentration measured by ACSM. The  
27 transported aerosol flow was split and directed to a scanning mobility particle sizer (model  
28 19.3.09 IFT/TT (TROPOS, Leipzig, Germany) and to the ACSM. In the ACSM particles were  
29 directed onto a resistively heated surface at ~600 °C where NR-PM<sub>1</sub> components are flash  
30 vaporized and the resulting gases are subsequently ionized by 70 eV electron impact. ACSM

1 was operated with a time resolution of ~28 min (for typical aerosol loadings, i.e., several  $\mu\text{g}$   
2  $\text{m}^{-3}$ ) and a scan rate of  $220 \text{ ms amu}^{-1}$  from  $m/z$  10 to 140 (approximately 31.9 s per scan and  
3 1.126 s pause), 56 scans and data interval 30 min. The data acquisition software used was  
4 DAQ 1.4.4.4. The mass concentrations and mass spectra were processed using ACSM  
5 standard data analysis software (v 1.5.3.0).

6 The instrument was calibrated using ammonium sulphate and ammonium nitrate. The  
7 determined calibration parameters were response factor (RF)  $\text{RF}_{\text{NO}_3} = 2.75 \cdot 10^{-11}$  and relative  
8 ionization efficiency (RIE)  $\text{RIE}_{\text{NH}_4} = 6.16$ ,  $\text{RIE}_{\text{SO}_4} = 0.92$ . The  $\text{RIE}_{\text{Org}} = 1.4$ ,  $\text{RIE}_{\text{chl}} = 1.3$  were  
9 set as default. However, the ACSM collection efficiency varies depending on the acidity of  
10 aerosol particles, aerosol composition, and particle phase water (Matthew et al., 2008). Many  
11 atmospheric aerosol studies reported reasonable agreement and linear correlations were  
12 obtained with other measurements by using a collection efficiency of 0.5 (Aiken et al. 2009;  
13 Timonen et al. 2010). Middlebrook et al. (2012) had proposed a collection efficiency  
14 calculation method. The collection efficiency for each measurement and daily mean CE  
15 values were calculated. The CE variation was small during the entire measurement campaign  
16 (March 2014), so the determined mean CE value was 0.52 with a standard deviation of 0.08,  
17 which is very close to other studies (Aiken et al. 2009; Timonen et al. 2010). This is not  
18 surprising because the sampled aerosol was dried to  $\text{RH} < 50\%$ ; moreover, the nitrate fraction  
19 was quite low (15% on average) and a high acidity of aerosols was not expected at Preila  
20 station (EMEP). Thus, we used the  $\text{CE} = 0.52$  in our investigation. The time series of organic  
21 aerosol mass spectra were processed using PMF analysis.

### 22 **2.2.2. PMF analysis**

23 The ACSM measured data were averaged to 1-hour time resolution. A graphical user interface  
24 SoFi (Source Finder) (Canonaco et al., 2013), developed at Paul Scherrer Institute was used to  
25 perform PMF for the source apportionment of the non-refractory OA mass spectra collected  
26 during March 2014. Only signals at  $m/z < 120$  were used for PMF analysis (Paatero and  
27 Tapper, 1994; Paatero, 1997) due to the following reasons: 1) the signals above  $m/z > 120$   
28 account for a minor fraction of total signal, 2) the  $m/z$ 's  $> 120$  have larger uncertainties  
29 because of poor ion transmission and the large interferences of naphthalene signals on some  
30  $m/z$ 's (e.g.,  $m/z$  127, 128, and 129) (Sun et al., 2012). A 2-factor solution including a Primary  
31 Organic Aerosol factor (POA), and a Secondary Organic Aerosol factor (SOA) was selected  
32 for this study. 20 different PMF runs were performed using a bootstrapping approach

1 (Davison and Hinkley, 1997). The bootstrap creates new input data matrices by randomly  
2 resampling measured mass spectra from the original input matrices. Moreover, each PMF  
3 bootstrap run is initiated from a different pseudorandom starting-point of the algorithm (seed).  
4 The bootstrapping approach, together with the seed approach allows a reasonable exploration  
5 of the PMF solution space (Paatero et al., 2014). Higher order solutions (3 factors) were  
6 explored yielding additional primary profiles, without a significant modification of the  
7 secondary contributions. Moreover the retrieved additional profiles showed very high time  
8 correlation ( $R^2 = 0.98$ ) with the POA factor, suggesting a splitting of the same aerosol source.  
9 As the additional primary factors could not be associated to specific primary emissions, those  
10 solutions are not shown. Medium-long range transport of polluted air masses resulted in a co-  
11 variability of the sources at the sampling site, hampering a further separation of the primary  
12 organic aerosols.

### 13 **2.2.3. 7-wavelength aethalometer and Scanning Mobility Particle Sizer**

14 An aethalometer, Model AE31 Spectrum (Manufactured by Aerosol d.o.o., Ljubljana,  
15 Slovenia) provided continuous measurements of the black carbon (BC) mass concentrations.  
16 The aethalometer was equipped with a PM<sub>2.5</sub> impactor. The aethalometer data were recorded  
17 with a 5-minute time resolution. The optical transmission of light absorbing carbonaceous  
18 aerosol particles was measured at seven wavelengths (370, 450, 520, 590, 660, 880, and 950  
19 nm). Measurements at 880 nm wavelength were used to determine BC mass concentration  
20 (Lavanchy et al., 1999). The aethalometer converts light attenuation measurements to BC  
21 mass using a specific attenuation absorption cross-section ( $\sigma$ ) of  $16.6 \text{ m}^2 \text{ g}^{-1}$  (at 880 nm)  
22 (Aethalometer Operations manual). The default value for the near-infrared wavelength of 880  
23 nm was set by the manufacturer. An empirical algorithm for loading effects compensation  
24 was used (Collaud Coen et al., 2010). [The](#) Ångström exponent of the absorption coefficient  
25 computed by fitting an exponential curve was evaluated.

26 Aerosol size distribution measurements were performed using a Scanning Mobility  
27 Particle Sizer (SMPS) model 19.3.09 IFT/TT (TROPOS, Leipzig, Germany), with automatic  
28 sheath flow, temperature and relative humidity (RH) control (SMPS setup V2.6 TT 2006) as  
29 described in Wiedensohler et al. (2012) applying a CPC UF-02M (Mordas et al., 2013). The  
30 SMPS measured particle size (8.7 to 840.0 nm) with a time resolution of 5 min having 72  
31 channels.

#### 2.2.4. OC/EC, $^{14}\text{C}$ , $\delta^{13}\text{C}$ and $\delta^{15}\text{N}$ analysis

Filter measurements were performed to determine OC, EC and total carbon (TC) concentrations with a thermo-optical OC/EC analyser (Sunset Laboratory Inc, USA) equipped with a non-dispersive infrared (NDIR) detector. A  $1.5\text{ cm}^2$  filter punch was analysed according to the EUSAAR2 protocol (Cavalli et al., 2010). The blank filter was subtracted only from the measured OC and TC concentrations, as for the EC the corresponding blank was below the detection limit of the instrument.

$^{14}\text{C}$  in EC and TC was measured using the accelerator mass spectrometer MICADAS, equipped with a gas-capable ion source (Szidat et al., 2014).  $^{14}\text{C}$  analysis of TC was determined after combustion of filter punches in an elemental analyser, directly coupled to the MICADAS (Salazar et al., 2015). The TC  $^{14}\text{C}$  raw data were corrected for a representative field blank. For  $^{14}\text{C}$  analysis of EC, the filters were first water extracted in order to minimize charring by removing the water-soluble OC (WSOC). Then the Swiss\_4S protocol (Zhang et al., 2012) was used to remove the water-insoluble OC (WINSOC) and measure the EC  $^{14}\text{C}$ , by coupling of the Sunset instrument to the MICADAS (Agrios et al., 2015).  $^{14}\text{C}$  in OC was determined from the TC  $^{14}\text{C}$  and the EC  $^{14}\text{C}$  results with an isotope mass balance calculation.

All the data from the  $^{14}\text{C}$  analysis were corrected for the decay of the  $^{14}\text{C}$  from 1950 until present. The reported uncertainty for the non-fossil fraction of EC includes both charring of OC (overestimation of EC) and EC loss (underestimation of EC) during the WINSOC removal process (Zhang et al., 2012). Non-fossil fractions of TC, EC and OC (i.e.,  $\text{TC}_{\text{nf}}$ ,  $\text{EC}_{\text{nf}}$  and  $\text{OC}_{\text{nf}}$ ) were determined from the individual  $^{14}\text{C}$  analyses and  $^{14}\text{C}$  reference values. These reference values represent emissions from purely non-fossil sources and amount to  $1.06 \pm 0.03$  for TC and OC and  $1.10 \pm 0.03$  for EC based on the calculation of Mohr et al. (2009). The fossil fractions of TC, EC and OC (i.e.,  $\text{TC}_{\text{f}}$ ,  $\text{EC}_{\text{f}}$  and  $\text{OC}_{\text{f}}$ ) were determined by subtraction of the respective non-fossil fractions.

Bulk  $\delta^{13}\text{C}$  and  $\delta^{15}\text{N}$  values were derived by measuring filter pieces ( $1.4\text{ cm}^2$ ) wrapped in tin capsules ( $8 \times 5\text{ mm}$ , Elemental Microanalysis) using an elemental analyser accompanying an isotope ratio mass spectrometer (EA-IRMS, Flash EA1112—Thermo V Advantage) via a ConFlo III interface. The autosampler of the EA was continuously flushed with He ( $180\text{ mL min}^{-1}$ ) to remove all atmospheric gases. Helium flow on the oxidation column was  $80\text{ mL min}^{-1}$ . Flash combustion occurred in the oxidation column with the presence of  $\text{O}_2$  (the  $\text{O}_2$  flow was  $180\text{ mL min}^{-1}$  for 4 s). Formed gases were taken to the reduction column in which molecular nitrogen was obtained from any nitrogen oxides followed by a water trap

1 (magnesium perchlorate). The nitrogen and the carbon dioxide were separated on a packed  
2 gas chromatographic (GC) column (PoraPlot, 3m\*2cm, 35 °C) and delivered to the isotope  
3 ratio mass spectrometer (via the ConFlo interface) where the measurement of carbon and  
4 nitrogen isotope ratio was made. The amount of nitrogen and carbon in the sample was  
5 determined by a thermal conductivity detector which is a part of the elemental analyser. These  
6 measurements were used in the isotope mass balance calculations (Eq. 1).

7 The total carbon and total nitrogen fractions of the aerosol particles were used for the isotopic  
8 ratio measurements. Stable carbon and nitrogen isotopic ratio measurements were expressed  
9 relative to the Vienna Pee Dee Belemnite (VPDB) standard using the formula:

$$10 \quad \delta^{13}C = \left( \frac{R_{\text{sample}}}{R_{\text{standard}}} - 1 \right) * 1000 (\text{‰}), \quad (1)$$

11 where  $R_{\text{sample}}$  and  $R_{\text{standard}}$  are the ratios of  $^{13}\text{C}$  to  $^{12}\text{C}$  (or  $^{15}\text{N}$  to  $^{14}\text{N}$ ) in the sample and the  
12 standard (referred to as VPDB), respectively.

13 Repeated analysis of certified reference material (caffeine IAEA-600) and oil (NBS 22) gave  
14 an average  $\delta^{13}\text{C}$  value: mean  $\pm \sigma = -27.77 \pm 0.08 \text{ ‰}$  (certified value: mean  $\pm \sigma = -27.771 \pm$   
15  $0.043 \text{ ‰}_{\text{VPDB}}$ ) and  $-30.03 \pm 0.09 \text{ ‰}$  (certified value: mean  $\pm \sigma = -30.031 \pm 0.043 \text{ ‰}_{\text{VPDB}}$ ),  
16 respectively. These values were used for  $\delta^{13}\text{C}$  measurements in order to evaluate an analytical  
17 precision and calibration of a reference gas ( $\text{CO}_2$ ) to VPDB. Meanwhile, the IAEA-600  
18 standard gave an average  $\delta^{15}\text{N}$  value: mean  $\pm \sigma = 1.0 \pm 0.2 \text{ ‰}$  which was used for calibration  
19 of a reference gas ( $\text{N}_2$ ) to air (for  $\delta^{15}\text{N}$  measurements).

20 Stable carbon and nitrogen isotope ratios were measured in the samples with the signal  
21 intensity reaching 1000 mV or more, due to analytical restrictions (the isotope values  
22 measurements below 1000 mV did not fulfil linearity requirements of 0.07 ‰/V for the  
23 internal standard).

24 The mass balance equation was used to calculate the real  $\delta$  values of carbon or nitrogen of the  
25 aerosol samples (blank correction):

$$26 \quad m_{\text{measured}} \times \delta X_{\text{measured}} = m_{\text{real}} \times \delta X_{\text{real}} + m_{\text{blank}} \times \delta X_{\text{blank}}, \quad (2)$$

27 where  $m_{\text{measured}}$  was the mass of measured material (carbon or nitrogen) in the measured  
28 sample,  $\delta X_{\text{measured}}$  was the measured (aerosol + filter)  $\delta$  value (carbon or nitrogen),  $m_{\text{real}}$  was  
29 the mass of real aerosol material (carbon or nitrogen),  $\delta X_{\text{real}}$  was the isotope ratio of the real  
30 aerosol material (carbon or nitrogen);  $m_{\text{blank}}$  and  $\delta X_{\text{blank}}$  were the mass and isotope ratio (of  
31 carbon or nitrogen) of the blank filter, respectively.

### 2.2.5. Radiocarbon-based source apportionment of carbonaceous aerosols

An estimate of fossil and non-fossil primary and secondary organic carbon ( $POC_f$ ,  $POC_{nf}$ ,  $SOC_f$ ,  $SOC_{nf}$ ) was achieved by coupling ACSM-PMF results,  $^{14}C$  data, and organic marker measurements using a chemical mass balance-like approach. The sensitivity of  $POC_f$ ,  $POC_{nf}$ ,  $SOC_f$ , and  $SOC_{nf}$  contributions to the assumed parameters and measurement errors are described in details in this section. The approach is based on the  $POC_{nf}$  estimate, for a subsequent determination of  $SOC_{nf}$ ,  $SOC_f$ , and  $POC_f$  as follows:

$$SOC_{nf} = OC_{nf} - POC_{nf} \quad (3)$$

$$SOC_f = SOC - SOC_{nf} \quad (4)$$

$$POC_f = OC_f - SOC_f \quad (5)$$

$^{14}C$  measurements and ACSM-PMF results were coupled as follows. Daily  $OC_{nf}$  measurements from radiocarbon analysis as well as average daily POA from ACSM-PMF results provided two upper boundaries for the daily  $POC_{nf}$  contribution. In this manner we identified a possible daily range of  $POC_{nf}$  contributions. In order to determine more precisely the  $POC_{nf}$  daily contributions within the aforementioned possible daily ranges, we performed a sensitivity analysis. Briefly, in the sensitivity analysis we considered a uniform distribution of possible  $POC_{nf}$  contributions within the identified possible daily ranges, meaning that each  $POC_{nf}$  value in the selected ranges was considered as equally probable (however, as discussed in the next section, in order to explore the influence of this assumption we also performed the same sensitivity analysis assuming a non-uniform distribution). Assuming no  $POC_{nf}$  contribution from other sources than biomass burning organic carbon (BBOC), each  $POC_{nf}$  contribution in the acceptable daily ranges could be written either as  $[BBOC] = [levoglucosan]/\alpha$  or as  $[BBOC] = [EC_{nf}]/\beta$ , where  $\alpha$  represents the levoglucosan/BBOC ratio and  $\beta$  represents the  $EC_{nf}$ /BBOC ratio. In two separated sensitivity analyses we scanned broad  $\alpha$  and  $\beta$  ranges covering the possible  $POC_{nf}$  daily ranges and we retained only  $POC_{nf}$ ,  $[levoglucosan]/\alpha$ , and  $[EC_{nf}]/\beta$  combinations associated to selected acceptance criteria described in the following. From the acceptable solutions we then derived the daily probability distribution function of  $POC_f$ ,  $SOC_{nf}$ ,  $SOC_f$ ,  $POC_f$ ,  $\alpha$ , and  $\beta$ .

The assumption that each input  $POC_{nf}$  contribution in the selected possible range is equally probable (hereafter referred to as “uniform distribution approach”) has advantages and

1 drawbacks: while this assumption doesn't consider any a priori information about  
 2 levoglucosan/POC<sub>nf</sub> and EC<sub>nf</sub>/POC<sub>nf</sub>, it considers those ratios as equally possible. To explore  
 3 the influence of this assumption on our results we performed the same sensitivity analysis  
 4 assuming an input levoglucosan/POC<sub>nf</sub> distribution derived from 33 profiles for combustion  
 5 of hard or softwoods in domestic fireplaces or woodstoves (Fine et al. 2001, 2002, 2004a,  
 6 2004b; Schmidl et al. 2008, the approach is hereafter referred to as “non-uniform distribution  
 7 approach”). We eventually derived the probability distribution functions of the  
 8 levoglucosan/POC<sub>nf</sub> and EC<sub>nf</sub>/POC<sub>nf</sub> ratios relative to the acceptable solutions. The two  
 9 approaches provided similar results. From the uniform distribution approach, a median  
 10 levoglucosan/POC<sub>nf</sub> ratio of 0.18 (1<sup>st</sup> quartile = 0.14; 3<sup>rd</sup> quartile = 0.23) and a median  
 11 EC<sub>nf</sub>/POC<sub>nf</sub> ratio of 0.32 (1<sup>st</sup> quartile = 0.28; 3<sup>rd</sup> quartile = 0.36) were retrieved, whilst from  
 12 the non-uniform distribution approach a median levoglucosan/POC<sub>nf</sub> ratio of 0.15 (1<sup>st</sup> quartile  
 13 = 0.13; 3<sup>rd</sup> quartile = 0.18) and a median EC<sub>nf</sub>/POC<sub>nf</sub> ratio of 0.33 (1<sup>st</sup> quartile = 0.28; 3<sup>rd</sup>  
 14 quartile = 0.36) were obtained.

15 In the following section a technical description of the sensitivity analysis implementation is  
 16 reported. For each filter sample  $i$ , 10000 random combinations ( $r$ ) of input data,  $[TC]_{i,r}$ ,  
 17  $[EC]_{i,r}$ ,  $[EC_f]_{i,r}$ ,  $[OC_f]_{i,r}$ , and  $[Levoglucosan]_{i,r}$ , were generated. In this process, we assume a  
 18 normal distribution of the errors around the average  $[X]_i$  value ( $X$  being one of the input  
 19 values mentioned above), and a distribution width equal to the standard deviation  $\sigma[X]_i$ :

20 For each random combination of input data, the corresponding  $[OC]_{i,r}$ ,  $[EC_{nf}]_{i,r}$ , and  $[OC_{nf}]_{i,r}$   
 21 values were determined as:

$$22 \quad [OC]_{i,r} = [TC]_{i,r} - [EC]_{i,r}, \quad (6)$$

$$23 \quad [EC_{nf}]_{i,r} = [EC]_{i,r} - [EC_f]_{i,r}, \quad (7)$$

$$24 \quad [OC_{nf}]_{i,r} = [OC]_{i,r} - [OC_f]_{i,r}. \quad (8)$$

25 10000 random  $[SOC]_s$  values were generated by randomly selecting a daily average  $[SOA]_s$   
 26 value from one of the 20 ACSM-PMF runs ( $s$ ). The corresponding  $[SOC]_s$  values were  
 27 derived as:

$$28 \quad [SOC]_s = [SOA]_s / (OM/OC)_{SOA(s)} \quad (9)$$

29  $(OM/OC)_{SOA(s)}$  and  $\sigma(OM/OC)_{SOA(s)}$  were calculated according to Aiken et al. (2009) as  
 30 function of the fractional contribution of the  $m/z$  44 ( $f_{44}$ ) to the  $SOA_s$  mass spectra. Fröhlich  
 31 et al. (2015) showed a systematic difference between  $f_{44}$  measured from ACSM and AMS;

Deleted: .

1 therefore an empirical correction factor was accordingly applied to rescale  $f44$  from ACSM  
 2 ( $f44_{ACSM}$ ) data to the corresponding AMS  $f44$  value ( $f44_{AMS}$ ). The uncertainty relative to the  
 3  $f44$  correction factor was propagated into  $\sigma(OM/OC)_{SOA(s)}$  which includes the  $O/C_s$   
 4 uncertainty as well. Each  $[SOC]_{i,r}$  value was obtained by randomly varying  $[SOC]_s$  assuming  
 5 a normal distribution of errors around the average value  $[SOC]_s$  and a distribution width equal  
 6 to  $\sigma(OM/OC)_{SOA(s)}$ .  $[BBOC]_{i,r}$  contributions for each sample  $i$  were derived as follows:

$$7 \quad [BBOC]_{i,r} = [levoglucosan]_{i,r}/\alpha, \quad (10)$$

$$8 \quad [BBOC]_{i,r} = [EC_{nf}]_{i,r}/\beta, \quad (11)$$

9 where  $\alpha$  represents the levoglucosan/BBOC ratio. This ratio was systematically varied  
 10 between 0.01 and 0.31 according to Huang et al. (2014) and references therein (scan step  
 11 equals 0.01).  $\beta$  corresponds to the EC/BBOC ratio. Values of  $\beta$  were systematically varied  
 12 between 0.1 and 0.4 according to Zhang et al. (2015) and references therein (scan step equal  
 13 to 0.01). 10000  $[BBOC]_{i,r,\alpha}$  and 10000  $[BBOC]_{i,r,\beta}$  were determined as in Eq. (8) and (9). Only  
 14 acceptable  $[BBOC]_{i,r,\alpha/\beta}$  ( $= [POC_{nf}]_{i,r,\alpha/\beta}$ ) values were considered for the sensitivity analysis.  
 15 The criteria to consider a  $[BBOC]_{i,r,\alpha/\beta}$  value as acceptable were:

$$16 \quad a) [BBOC]_{i,r,\alpha/\beta} \leq [POC]_{i,r} \text{ and } b) [BBOC]_{i,r,\alpha/\beta} \leq [OC_{nf}]_{i,r} \quad (12)$$

17  $[POC]_{i,r}$  was determined as follows:

$$18 \quad [POC]_{i,r} = [OC]_{i,r} - [SOC]_{i,r}, \quad (13)$$

19 Only acceptable  $[POC]_{i,r}$  values were considered. The criterion to consider a  $[POC]_{i,r}$  value as  
 20 acceptable was:

$$21 \quad c) [POA]_s/[POC]_{i,r} \geq 1.3 \text{ according to Mohr et al. (2009), Aiken et al. (2009).}$$

22  $[SOC_{nf}]_{i,r}$  values were then derived as:

$$23 \quad [SOC_{nf}]_{i,r} = [OC_{nf}]_{i,r} - [POC_{nf}]_{i,r} \quad (14)$$

24 Only acceptable  $[SOC_{nf}]_{i,r}$  values were considered, where

$$25 \quad d) [SOC_{nf}]_{i,r} \leq [SOC]_{i,r} \quad (15)$$

26 Only solutions where all 4 criteria a), b), c), and d) held were considered acceptable and  
 27 retained.

28 Finally,  $[SOC_f]_{i,r}$  and  $[POC_f]_{i,r}$  were calculated as:

$$29 \quad [SOC_f]_{i,r} = [SOC]_{i,r} - [SOC_{nf}]_{i,r}, \quad (16)$$

1  $[\text{POC}]_{i,t} = [\text{OC}]_{i,t} - [\text{SOC}]_{i,t}$ . (17)

2 **2.2.6. Organic markers and satellite products**

3 Determination of organic marker concentrations was performed using a developed in-situ  
4 derivatization thermal desorption gas chromatography time of flight mass spectrometry  
5 (IDTD-GC-MS) method (Orasche et al., 2011).

6 Biomass burning episodes were explored using a variety of remote sensing datasets and their  
7 derived properties. Satellite data and ground based observations of aerosol properties from the  
8 MODIS, HYSPLIT and SILAM (Sofiev et al., 2006) were coupled to analyse the variability  
9 of carbonaceous aerosols in Lithuania (Fig. 2).

10 The MODIS sensors on-board NASA's Terra and Aqua satellites provide multiple thermal  
11 observations of the Earth on 9–10 March 2014 at a spatial resolution of 1 km using the latest  
12 version of the MODIS Active Fire Product (MOD14/MYD14) algorithm (MODIS, 2011). To  
13 identify the influence of air masses from different transport pathways on the large biomass  
14 burning (BB) event occurring at Preila, 72-h back trajectories at an arrival height of 100, 200  
15 and 500 m were calculated by the Hybrid Single Particle Lagrangian Integrated Trajectory  
16 (HYSPLIT) Model Version 4.8 (Stein et al., 2015). All air mass back trajectories were  
17 generated using Gridded Meteorological Data archives of the Air Resource Laboratory  
18 (ARL), National Ocean and Atmospheric Administration (NOAA) (Fig. 2A).

19 The Navy Aerosol Analysis and Prediction System (NAAPS) model results were used to  
20 define the distribution of BB aerosols from wildfire areas (model description and results are  
21 available from the web pages of the Naval Research Laboratory, Monterey, CA, USA;  
22 <http://www.nrlmry.navy.mil/aerosol/>) (Fig. 2B). The NAAPS model has been adapted to  
23 combine real-time observations of biomass burning based on the joint Navy/NASA/NOAA  
24 Fire Locating and Modelling of Burning Emissions system (FLAMBE,  
25 <http://www.nrlmry.navy.mil/flambe/>) (Reid et al., 2004). The method has proven helpful in  
26 previous studies of long-range and regional transport of smoke (Honrath et al., 2004). The  
27 resolution of 2.5° longitude × 2.5° latitude National Centers for Environmental Prediction  
28 (NCEP) reanalysis data (Kanamitsu et al., 2002) during the grass burning episode were  
29 analysed to illustrate the sub synoptic-scale weather feature among the biomass burning  
30 events over Lithuania issued every 6 h for March 2014 (Fig. 2C). SILAM is an air quality and  
31 emergency open code system (<http://silam.fmi.fi/>) providing PM<sub>2.5</sub> emission maps by Eulerian  
32 dynamics and a combination of basic acid and ozone chemistry with inert particles for fire

1 and anthropogenic primary PM emission to account for the fire induced aerosol contribution  
2 (Fig. 2D).

### 3 **3. Results and discussion**

#### 4 **3.1 Identification of grass burning event**

5 Massive active fires occurred throughout the Kaliningrad region (Russia), Belorussia and  
6 Ukraine (Fig. 2A) when a high atmospheric pressure system was situated over the study area,  
7 as illustrated in the weather map of Fig. 2C. The plumes from those fires covered a large area  
8 south of the Baltic region and were transported thousands of kilometres downwind affecting  
9 the background air in Lithuania (Fig. 2). Although the number of fires was similar to [that in](#)  
10 [previous years](#), the impact of the fire events on the Lithuanian air quality was enhanced in  
11 March 2014 due to air mass transport of smoke entrained in deep convection by the large  
12 scale circulation around the pressure maximum of the anticyclonic system (Fig. 2C). This is  
13 consistent with the relatively high concentrations of smoke reaching Preila as predicted by  
14 NAAPS (Fig. 2B).

15 The weather maps showed that the high concentration of pollutants during this BB event was  
16 caused by the anticyclonic large-scale movement, which persisted throughout the lower  
17 troposphere causing stagnant conditions and extended aerosol residence time.

#### 18 **3.2 Investigation of PM<sub>1</sub> composition and ambient concentrations of** 19 **organic tracers**

20 The climatic conditions in West Europe as well as in [the western part of Lithuania are](#)  
21 [moderate](#), warm climate dominating by air mass transport from Atlantic Ocean, leading to  
22 higher humidity. Annual mean temperature increases in west-east direction. The average  
23 temperature of March was ~3–4 °C. During the BB event (9–11 March) combustion products  
24 were spread over the study region by the large-scale atmospheric circulation processes. At the  
25 beginning of the BB episode, the wind speed was up to 3 m s<sup>-1</sup> on average in the daytime of  
26 9<sup>th</sup> March, causing weaker dilution of the pollutants while the BC concentration was higher  
27 than 12 µg m<sup>-3</sup>.

28 During the campaign, on average, organic aerosol (46%, 3.2 µg m<sup>-3</sup> (σ = 4.8 µg m<sup>-3</sup>))  
29 constituted the major fraction of the NR-PM<sub>1</sub> aerosol concentration composition measured by  
30 ACSM with lower contributions of sulfate (17%, 1.2 µg m<sup>-3</sup> (σ = 1.1 µg m<sup>-3</sup>)), nitrate (20%,

Deleted: to previous years

Deleted: in west part of Lithuania are moderate

1 1.4  $\mu\text{g m}^{-3}$  ( $\sigma = 1.8 \mu\text{g m}^{-3}$ ), ammonium (15%, 1.0  $\mu\text{g m}^{-3}$  ( $\sigma = 0.9 \mu\text{g m}^{-3}$ )), and chloride  
2 (2%, 0.1  $\mu\text{g m}^{-3}$  ( $\sigma = 0.3 \mu\text{g m}^{-3}$ )). The average composition of NR-PM<sub>1</sub> showed similar  
3 dominance of organics to previous observations in Europe (e.g., Crippa et al., 2014). OA  
4 contribution to NR-PM<sub>1</sub> was found to be much higher during the grass burning period (61%,  
5 8.6  $\mu\text{g m}^{-3}$  ( $\sigma = 5.0 \mu\text{g m}^{-3}$ )), followed by sulfate (5%, 1.4  $\mu\text{g m}^{-3}$  ( $\sigma = 0.5 \mu\text{g m}^{-3}$ )), nitrate  
6 (19%, 3.0  $\mu\text{g m}^{-3}$  ( $\sigma = 1.4 \mu\text{g m}^{-3}$ )), ammonium (13%, 1.6  $\mu\text{g m}^{-3}$  ( $\sigma = 0.7 \mu\text{g m}^{-3}$ )), and  
7 chloride (3%, 0.4  $\mu\text{g m}^{-3}$  ( $\sigma = 0.3 \mu\text{g m}^{-3}$ )) (Fig. 5A).

8 The concentrations of the monosaccharide anhydrides together with those of OC and EC are  
9 presented in Fig. 3. It is evident that during the event, when grass burning was most intense,  
10 the levoglucosan concentration increased up to 680  $\text{ng m}^{-3}$ . That is substantially lower than  
11 values reported during the extreme event of August 2010 in Moscow – 3100  $\text{ng m}^{-3}$   
12 (Popovicheva et al., 2014) and is higher than values (220–290  $\text{ng m}^{-3}$ ) reported during a  
13 major biomass burning episode over northern Europe in Helsinki (Saarikoski et al., 2007),  
14 while background values in Nordic rural background sites were found to be 2.1–9.8  $\text{ng m}^{-3}$   
15 (Yttri et al., 2011). Concentrations of mannosan varied from 3.1 to 68.0  $\text{ng m}^{-3}$  and those of  
16 galactosan from 1.0 to 12.0  $\text{ng m}^{-3}$ . The levoglucosan to mannosan (L/M), levoglucosan to  
17 galactosan (L/G) and levoglucosan to OC (L/OC) ratios were used before to separate different  
18 BB sources (Fabbri et al., 2009; Oanh et al., 2011; Harrison et al., 2012). We measured  
19 average L/M and L/G ratios of 16.4 and 135.8, respectively. This is similar to the values  
20 found by Orasche et al. (2012) from wood combustion in residential wood appliances and in  
21 the range of L/M ratios reported (2.0–33.3) for grass fires by Oros et al. (2006). Excluding the  
22 strong event days of March 9 and 10 the sugars showed a good correlation with each other ( $R^2$   
23  $> 0.86$ ). On March 9 and 10 the mannosan/galactosan was lower at 2–6, indicating a different  
24 source than on the other days. Low mannosan/galactosan ratios were observed for grass and  
25 leaves (Sullivan et al., 2014). We observed an L to OC ratio from 0.06 to 0.16 during the  
26 biomass burning period and of  $\sim 0.03$  during the days without biomass burning events. The  
27 values observed during biomass burning are in the range of those (0.04–0.20) reported for  
28 wildland fuels (Sullivan et al., 2008). The OC/EC ratio ranged from 1.5 to 6.2 being lower on  
29 event days (2.4–3.0) indicating an aerosol composition dominated by organic aerosol. During  
30 the intensive grass burning episode, consecutive new particle formation (NPF) events were  
31 observed. [The observed NPF events](#) could be attributed to the grass burning and secondary  
32 biomass burning product transformation as was evaluated in earlier studies over the same area

Deleted: Observed NPF

1 (Ulevicius et al., 2010b). At 13:00, there was significant new particle formation on 9<sup>th</sup> and  
2 10<sup>th</sup> March followed by subsequent growth up to three hours. A total particle number  
3 concentration with a daily mean value of 6440 cm<sup>-3</sup> (with maximum value of 13000 cm<sup>-3</sup>) was  
4 observed, which was extremely much higher than the daily mean observations in non-event  
5 days (1660 cm<sup>-3</sup>). In this area an annual mean total particle concentration of 2650 cm<sup>-3</sup> was  
6 observed (Byčėnkiėnė et al., 2013). Non-event days were characterized by bimodal (Aitken  
7 (geometric mean diameter ( $D_g$ ) of 44 nm) and accumulation ( $D_g = 128$  nm)) distributions with  
8 a standard deviation of 1.68 and 1.87, respectively. In comparison, during the biomass  
9 burning event trimodal (nucleation ( $D_g = 9.0$  nm), Aitken ( $D_g = 31.0$  nm) and accumulation  
10 ( $D_g = 102$  nm)) distributions with a standart deviation of 1.77, 1.71 and 1.68, respectively.  
11 However, the volume distribution was characterized by a bimodal size distribution for the  
12 non-event days ( $D_g = 330$  and 665 nm) and for the event day ( $D_g = 250$  and 590 nm).  
13 The measured  $\delta^{13}\text{C}$  values varied from -28.2 to -26.7 ‰. The lowest stable carbon isotope  
14 ratio values (-28.5 ‰) were detected during the period with the highest total carbon  
15 concentration of 12.2  $\mu\text{g m}^{-3}$  (2014.03.10) and 8.5  $\mu\text{g m}^{-3}$  (2014.03.09). The highest  
16 concentration 14.0  $\mu\text{g m}^{-3}$  of nitrogen was detected on 10 March 2014. The nitrogen isotope  
17 ratio values varied from +1.0 to +13.0 ‰ (Fig. 4).  
18 Stable carbon and nitrogen isotope ratios values of aerosol particles derived from biomass  
19 burning (C3 plants) and liquid fossil fuel are overlapping (Garbaras et al., 2015; Masalaite et  
20 al., 2015; Turekian et al., 1998). Coal derived aerosol particles are characterised by higher  
21  $\delta^{13}\text{C}$  and lower  $\delta^{15}\text{N}$  values (Fig. 4, solid lines).  $\delta^{13}\text{C}$  values of aerosol particles during wild  
22 grass burning events distinguish in low  $\delta^{13}\text{C}$  values (Garbaras et al., 2008; Ulevicius et. al.,  
23 2010b). The above mentioned distribution of  $\delta^{13}\text{C}$  and  $\delta^{15}\text{N}$  values allowed excluding coal  
24 burning as main source for aerosol particles at Preila during the investigated event. Aerosol  
25 particles with  $\delta^{13}\text{C}$  values equal to -28 ‰ and below originated mainly from grass burning  
26 events. This interpretation of the data is consistent with the radiocarbon analysis shown  
27 below.

Deleted: The

Deleted: ,

Deleted: ,

### 28 3.3 Source apportionment of EC and OC using <sup>14</sup>C data

29 Relative fossil and non-fossil contributions to OC and EC were evaluated using <sup>14</sup>C  
30 analysis (Szidat et al., 2014) to enable a more detailed source attribution of the carbonaceous  
31 aerosol mass. Widely used, two-source simple models (Currie, 2000; Lemire et al., 2002;  
32 Lewis et al., 2004; Szidat et al., 2004) can only distinguish fossil from non-fossil TC

1 emissions. Here, carbonaceous aerosol was described to be composed of the following 4  
2 categories:  $OC_f$  and  $EC_f$  attributed to primary and secondary fossil fuel combustion; and  $OC_{nf}$ ,  
3 and  $EC_{nf}$  typically attributed to primary and secondary biomass burning, cooking, biogenic  
4 emissions and non-fossil OC combustion (Table 2, Fig. 5). There was day-to-day variation in  
5 the fractional contributions to TC throughout the BB event. The fraction of elemental carbon  
6 from biomass burning  $EC_{bb}$  ( $= EC_{nf}$ ) to total EC was found to be on average  $67 \pm 3\%$ . For  $EC_{bb}$   
7 the mean relative contribution to total carbon in background areas of Northern countries was  
8 found to be  $<1.5\%$  on non-event days (Yttri et al., 2011). It was also reported that a major  
9 peak in  $EC_{bb}$  values between March and April was observed at the Zeppelin atmospheric  
10 observatory (Yttri et al., 2014). Observed high values are unusual and have only been found  
11 in wood burning dominated places like villages in Alpine valleys (Zotter et al., 2014). This  
12 shows, together with the high levels of levoglucosan, that biomass burning contributed to a  
13 large extent to  $OC_{nf}$  during this event. A mean light absorption coefficient  $\alpha_{370-950}$  (the  
14 absorption exponent calculated using the seven wavelengths Aethalometer) of 1.38 ( $\sigma = 0.11$ )  
15 was obtained during wildfires, which is higher than the mean  $\alpha_{370-950}$  calculated for the non-  
16 event days (1.13,  $\sigma = 0.19$ ). The light absorption exponent values were calculated with  $\lambda =$   
17 370 – 520 nm and  $\lambda = 590 - 950$  nm wavelengths for comparison purpose. The mean values of  
18  $\alpha_{370-520}$  and  $\alpha_{590-950}$  were found to be 1.53 ( $\sigma = 0.19$ ) and 1.32 ( $\sigma = 0.09$ ) during event days  
19 and 1.25 ( $\sigma = 0.27$ ) and 1.13 ( $\sigma = 0.18$ ) for the non-event days, respectively. In comparison,  
20 during a similar event in Preila higher mean values of  $\alpha_{370-520}$  and  $\alpha_{590-950}$  nm were observed  
21 (2.4 ( $\sigma = 0.1$ ) and 1.5 ( $\sigma = 0.1$ ), respectively) in 2008, as well as during the event in 2009 (2.3  
22 ( $\sigma = 0.1$ ) and 1.6 ( $\sigma = 0.1$ ), respectively) (Ulevicius et al., 2010a). This is an indication of the  
23 influence of the biomass burning on the Ångström exponent of the absorption coefficient  $\alpha$ .  
24 The impact of organic aerosols on the spectral dependence of light absorption was already  
25 confirmed by the OC/EC ratios. PMF analysis of OA spectra resolved two OA components,  
26 which are attributed to POA and SOA, whose mass spectra and time series are presented in  
27 Fig. 5 B, C. Combining these results with the  $^{14}C$  measurements as described in section 2.2.4  
28 shows that the high grass burning pollution event is characterized by a high non-fossil organic  
29 compound fraction, which accounts for up to  $\sim 90\%$  of total carbon mass.

30 SOA showed reasonable correlation ( $R^2 = 0.62$ ) with average  $NH_4^+$  mass concentration during  
31 the BB event.  $NH_4^+$  is in this case a good tracer for secondary aerosol, as it correlates well  
32 with the sum of  $NO_3^-$  and  $SO_4^{2-}$  ( $R^2 = 0.96$ ) (Fig. 6). There was day-to-day variation

Deleted: .

1 throughout the study period with the non-fossil contribution to organic carbon between 67–  
2 86%.  $OC_{nf}$  was estimated to be ~65% primary, while the primary fraction of the  $OC_f$  in Preila  
3 was estimated to be ~9%. Conversely, when  $EC_f$  showed a lower contribution (2014.03.07  
4 and 2014.03.10; 19% and 24%, respectively),  $OC_f$  was also lower (15%) (Table 3). The high  
5 fraction of biomass burning was corroborated by measurements of levoglucosan. Other  
6 molecular markers such as hopanes for traffic emissions and picene for coal combustion  
7 (Rutter et al., 2009) were also measured in order to monitor the possible contribution of fossil  
8 fuel combustion during the high pollution event. Although their concentrations increased  
9 during the episode, suggesting a contribution of co-transported fossil fuel combustion  
10 aerosols, the radiocarbon analysis revealed the contribution of this fraction to be minor ( $EC_f$   
11 ranged from 0.3 to 1.1  $\mu\text{g m}^{-3}$ ;  $OC_f$  ranged from 0.5 to 1.6  $\mu\text{g m}^{-3}$  (Fig. 5)). The  
12 concentrations of the molecular markers are provided in Table S1 of the Supplementary  
13 material. The combination of measurements and source apportionment techniques allowed a  
14 better characterization of the carbonaceous aerosol sources. POA determined with the ACSM  
15 is mostly non-fossil and originates from grass burning. It is shown that  $POC_{nf}$  and  $SOC_{nf}$   
16 concentrations increase drastically (from 1.1 to 5.4  $\mu\text{g m}^{-3}$  for  $POC_{nf}$ ; from 0.9 to 3.1  $\mu\text{g m}^{-3}$   
17 for  $SOC_{nf}$ ) with increasing influence of biomass burning, whereas the concentrations of the  
18 respective fossil fractions show a smaller increase during this episode. From the acceptable  
19 solutions obtained from the sensitivity test described in section 2.2.5, we derived the  
20 probability distribution functions of the different daily contributions for the  $POC_f$ ,  $SOC_{nf}$ ,  
21  $SOC_f$ ,  $POC_f$  fractions (Fig. 7). The median tests are consistent and EC/BBOC ratios obtained  
22 from the sensitivity tests are consistent with values reported in Zhang et al. (2015) and Huang  
23 et al. (2014) (Fig. 8).

24 In Zhang et al. (2015) agricultural waste combustion is considered to be the main contributor  
25 to the total biomass burning. Note that on 5 March a different Levoglucosan/BBOC ratio was  
26 found (0.31) compared to the non-event days (~0.15). Also, this is consistent with different air  
27 mass back-trajectories, associated to air masses originating in the Southern and Central  
28 Russian Federal districts, i.e., air masses with a different geographical origin and associated to  
29 potentially different types of biomass burning.

#### 30 **4 Conclusions**

31 In March 2014, an intensive field campaign was conducted in the marine background of  
32 the South Eastern Baltic region during a period of intensive grass burning. This paper

1 provides the biomass burning related aerosol concentrations during grass burning estimated  
2 by data that stem from a synthesis of various techniques including surface online/offline and  
3 satellite based measurements. Lidar vertical profiles allowed confirming smoke plumes from  
4 wild fire regions. Levels of source specific tracers, i.e., levoglucosan as well as  $^{14}\text{C}$  of TC, EC  
5 and OC were used as input for source apportionment of the carbonaceous aerosol. Overall, EC  
6 and OC were dominated by non-fossil sources. The total POC fraction was separated into  
7  $\text{POC}_f$  and  $\text{POC}_{nf}$ . In terms of OC mass,  $\text{POC}_{nf}$  contributes on average 56%, while the relative  
8 contribution to TC was found to be on average 39%. In case of SOC, the contribution of  $\text{OC}_f$   
9 reached on average 10.3% (non-fossil – 25%). The  $\delta^{13}\text{C}$  value of -28.5‰ indicated the  
10 dominance of the aerosol derived from the vegetation burning as no significant carbon isotope  
11 fractionation occurs between the aerosol particles from biomass burning and the raw biomass  
12 material.

### 13 **Acknowledgements**

14 This work was supported by the Lithuanian-Swiss Cooperation Programme “Research and  
15 Development” project AEROLIT (Nr. CH-3-ŠMM-01/08).

16

## 1 **References**

- 2 Agrios, K., Salazar, G. A., Zhang, Y. L., Uglietti, C., Battaglia, M., Luginbühl, M., Ciobanu,  
3 V. G., Vonwiller, M., and Szidat, S.: Online coupling of pure O<sub>2</sub> thermo-optical methods - <sup>14</sup>C  
4 AMS for source apportionment of carbonaceous aerosols study, *Nucl. Instrum. Meth. Phys.*  
5 *Res. B.*, 361, 288-293, doi:10.1016/j.nimb.2015.06.008, 2015.
- 6 Aiken, A. C., Salcedo, D., Cubison, M. J., Huffman, J. A., DeCarlo, P. F., Ulbrich, I. M.,  
7 Docherty, K. S., Sueper, D., Kimmel, J. R., Worsnop, D. R., Trimborn, A., Northway, M.,  
8 Stone, E. A., Schauer, J. J., Volkamer, R. M., Fortner, E., de Foy, B., Wang, J., Laskin, A.,  
9 Shutthanandan, V., Zheng, J., Zhang, R., Gaffney, J., Marley, N. A., Paredes-Miranda, G.,  
10 Arnott, W. P., Molina, L. T., Sosa, G., and Jimenez, J. L.: Mexico City aerosol analysis  
11 during MILAGRO using high resolution aerosol mass spectrometry at the urban supersite  
12 (T0) – Part 1: Fine particle composition and organic source apportionment, *Atmos. Chem.*  
13 *Phys.*, 9, 6633– 6653, doi:10.5194/acp-9-6633-2009, 2009.
- 14 Akagi, S. K., Craven, J. S., Taylor, J. W., McMeeking, G. R., Yokelson, R. J., Burling, I. R.,  
15 Urbanski, S. P., Wold, C. E., Seinfeld, J. H., Coe, H., Alvarado, M. J., and Weise, D. R.:  
16 Evolution of trace gases and particles emitted by a chaparral fire in California, *Atmos. Chem.*  
17 *Phys.*, 12, 1397–1421, doi:10.5194/acp-12-1397-2012, 2012.
- 18 Baldini, G., Campadelli, P., and Fradegrada, M.: Biomass burning monitoring by scene  
19 analysis, In *Proceedings of Visualization, Imaging, and Image Processing*, Calgary, 2002.
- 20 Baron, P. A. and Willeke, K. (Eds.): *Aerosol Measurement: Principles, Techniques, and*  
21 *Applications* 2nd Edition, Wiley, New York, 2001.
- 22 Beddows, D. C. S., Dall'Osto, M., Harrison, R. M., Kulmala, M., Asmi, A., Wiedensohler, A.,  
23 Laj, P., Fjaeraa, A. M., Sellegri, K., Birmili, W., Bukowiecki, N., Weingartner, E.,  
24 Baltensperger, U., Zdimal, V., Zikova, N., Putaud, J.-P., Marinoni, A., Tunved, P., Hansson,  
25 H.-C., Fiebig, M., Kivekäs, N., Swietlicki, E., Lihavainen, H., Asmi, E., Ulevicius, V., Aalto,  
26 P. P., Mihalopoulos, N., Kalivitis, N., Kalapov, I., Kiss, G., de Leeuw, G., Henzing, B.,  
27 O'Dowd, C., Jennings, S. G., Flentje, H., Meinhardt, F., Ries, L., Denier van der Gon, H. A.  
28 C., and Visschedijk, A. J. H.: Variations in tropospheric submicron particle size distributions  
29 across the European continent 2008–2009, *Atmos. Chem. Phys.*, 14, 4327-4348,  
30 doi:10.5194/acp-14-4327-2014, 2014.

1 Bougiatioti, A., Stavroulas, I., Kostenidou, E., Zampas, P., Theodosi, C., Kouvarakis, G.,  
2 Canonaco, F., Prévôt, A. S. H., Nenes, A., Pandis, S. N., and Mihalopoulos, N.: Processing of  
3 biomass-burning aerosol in the eastern Mediterranean during summertime, *Atmos. Chem.*  
4 *Phys.*, 14, 4793-4807, doi:10.5194/acp-14-4793-2014, 2014.

5 Byčėnkiene, S., Ulevicius, V., and Kecorius, S.: Characteristics of black carbon aerosol mass  
6 concentration over the East Baltic region from two-year measurements, *J. Environ. Monit.*,  
7 13(4), 1027–1038, doi: 10.1039/C0EM00480D, 2011.

8 Byčėnkiene, S., Ulevicius V., Dudoitis V., and Pauraitė J.: Identification and characterization  
9 of black carbon aerosol sources in the East Baltic region, *Adv. Meteor.*, 2013, Article ID  
10 380614, doi,org/10.1155/2013/380614, 2013.

11 Canonaco, F., Crippa, M., Slowik, J. G., Baltensperger, U., and Prevot A. S. H.: SoFi, an  
12 IGOR-based interface for the efficient use of the generalized multilinear engine (ME-2) for  
13 the source apportionment: ME-2 application to aerosol mass spectrometer data, *Atmos. Meas.*  
14 *Tech.*, 6(12), 3649-3661, 2013.

15 Capes, G., Johnson, B., McFiggans, G., Williams, P. I., Haywood, J., and Coe, H.: Aging of  
16 biomass burning aerosols over West Africa: aircraft measurements of chemical composition,  
17 microphysical properties, and emission ratios, *J. Geophys. Res. Atmos.*, 113, D00C15, doi:  
18 10.1029/2008JD009845, 2008.

19 Cavalli, F., Viana, M., Yttri, K. E., Genberg, J., and Putaud, J.-P.: Toward a standardised  
20 thermal-optical protocol for measuring atmospheric organic and elemental carbon: the  
21 EUSAAR protocol, *Atmos. Meas. Tech.*, 3, 79–89, doi:10.5194/amt-3-79-2010, 2010.

22 Ceburnis, D., Garbaras, A., Szidat, S., Rinaldi, M., Fahrni, S., Perron, N., Wacker, L., Leinert,  
23 S., Remeikis, V., Facchini, M. C., Prevot, A. S. H., Jennings, S. G., and O'Dowd, C. D.:  
24 Quantification of the carbonaceous matter origin in submicron marine aerosol particles by  
25 dual carbon isotope analysis, *Atmos. Chem. Phys.*, 11, 8593-8606, doi:10.5194/acp-11-8593-  
26 2011.

27 Collaud Coen, M., Weingartner, E., Apituley, A., Ceburnis, D., Fierz-Schmidhauser, R.,  
28 Flentje, H., Henzing, J. S., Jennings, S. G., Moerman, M., Petzold, A., Schmid, O., and  
29 Baltensperger, U.: Minimizing light absorption measurement artifacts of the Aethalometer:  
30 evaluation of five correction algorithms, *Atmos. Meas. Tech.*, 3, 457–474, doi: 10.5194/amt-  
31 3-457-2010, 2010.

1 Crippa, M., Canonaco, F., Lanz, V. A., Äijälä, M., Allan, J. D., Carbone, S., Capes, G.,  
2 Ceburnis, D., Dall'Osto, M., Day, D. A., DeCarlo, P. F., Ehn, M., Eriksson, A., Freney, E.,  
3 Hildebrandt Ruiz, L., Hillamo, R., Jimenez, J. L., Junninen, H., Kiendler-Scharr, A.,  
4 Kortelainen, A.-M., Kulmala, M., Laaksonen, A., Mensah, A. A., Mohr, C., Nemitz, E.,  
5 O'Dowd, C., Ovadnevaite, J., Pandis, S. N., Petäjä, T., Poulain, L., Saarikoski, S., Sellegri, K.,  
6 Swietlicki, E., Tiitta, P., Worsnop, D. R., Baltensperger, U., and Prévôt, A. S. H.: Organic  
7 aerosol components derived from 25 AMS data sets across Europe using a consistent ME-2  
8 based source apportionment approach, *Atmos. Chem. Phys.*, 14, 6159-6176, doi:10.5194/acp-  
9 14-6159-2014, 2014.

10 Crutzen, P. J., Heidt, L. E., Krasnec, J. P., Pollock, W. H., and Seiler, W.: Biomass burning as  
11 a source of atmospheric gases CO, H<sub>2</sub>, N<sub>2</sub>O, NO, CH<sub>3</sub>C1, and COS, *Nature* 282, 253-256,  
12 doi:10.1038/282253a0, 1979.

13 Currie, L. A.: Evolution and multidisciplinary frontiers of <sup>14</sup>C aerosol science, *Radiocarbon*  
14 42, 115–126, 2000.

15 Davison, A. C. and Hinkley, D. V.: *Bootstrap Methods and Their Application*, Cambridge  
16 University Press, Cambridge, UK, 582 pp., 1997.

17 EMEP (European Monitoring and Evaluation Programme), website:  
18 <http://www.emep.int/index.html>

19 Fabbri, D., Torri, C., Simoneit, B., Marynowski, L., Rushdi, A., and Fabianska, M.:  
20 Levoglucosan and other cellulose and lignin markers in emissions from burning of Miocene  
21 lignites, *Atmos. Environ.*, 43, 2286-2295, doi:10.1016/j.atmosenv.2009.01.030, 2009.

22 Fine, P. M., Cass, G. R., and Simoneit, B. R. T.: Chemical characterization of fine particle  
23 emissions from fireplace combustion of woods grown in the northeastern United States,  
24 *Environ. Sci. Technol.*, 35, 2665-2675, doi:10.1021/es001466k, 2001.

25 Fine, P. M., Cass, G. R., and Simoneit, B. R. T.: Chemical characterization of fine particle  
26 emissions from the fireplace combustion of woods grown in the southern United States,  
27 *Environ. Sci. Technol.*, 36, 1442-1451, doi: 10.1021/es0108988, 2002.

28 Fine, P. M., Cass, G. R., and Simoneit, B. R. T.: Chemical characterization of fine particle  
29 emissions from the wood stove combustion of prevalent United States tree species, *Environ.*  
30 *Eng. Sci.*, 21, 705-721, doi: 10.1089/ees.2004.21.705, 2004a.

1 Fine, P. M., Cass, G. R., and Simoneit, B. R. T.: Chemical characterization of fine particle  
2 emissions from fireplace combustion of woods grown in the Midwestern and Western United  
3 States, *Environ. Eng. Sci.*, 21, 387-409, doi: 10.1089/109287504323067021, 2004b.

4 Fröhlich, R., Crenn, V., Setyan, A., Belis, C. A., Canonaco, F., Favez, O., Riffault, V.,  
5 Slowik, J. G., Aas, W., Aijälä, M., Alastuey, A., Artiñano, B., Bonnaire, N., Bozzetti, C.,  
6 Bressi, M., Carbone, C., Coz, E., Croteau, P. L., Cubison, M. J., Esser-Gietl, J. K.,  
7 Green, D. C., Gros, V., Heikkinen, L., Herrmann, H., Jayne, J. T., Lunder, C. R.,  
8 Minguillón, M. C., Močnik, G., O'Dowd, C. D., Ovadnevaite, J., Petralia, E., Poulain, L.,  
9 Priestman, M., Ripoll, A., Sarda-Estève, R., Wiedensohler, A., Baltensperger, U., Sciare, J.,  
10 and Prévôt, A. S. H.: ACTRIS ACSM intercomparison – Part 2: Intercomparison of ME-2  
11 organic source apportionment results from 15 individual, co-located aerosol mass  
12 spectrometers, *Atmos. Meas. Tech.*, 8, 2555-2576, doi:10.5194/amt-8-2555-2015, 2015.

13 Garbaras, A., Andriejauskiene, J., Bariseviciute, R., and Remeikis, V.: Tracing of atmospheric  
14 aerosol sources using stable carbon isotopes, *Lith. J. Phys.*, 48, 259-264,  
15 doi:10.3952/lithjphys.48309, 2008.

16 Garbaras, A., Masalaite, A., Garbariene, I., Ceburnis, D., Krugly, E., Remeikis, V., Puida, E.,  
17 Kvietkus, K., and Martuzevicius, D.: Stable carbon fractionation in size segregated aerosol  
18 particles produced by controlled biomass burning, *J. Aerosol Science*, 79, 86-96,  
19 doi:10.1016/j.jaerosci.2014.10.005, 2015.

20 Grieshop, A. P., Logue, J. M., Donahue, N. M., and Robinson, A. L.: Laboratory investigation  
21 of photochemical oxidation of organic aerosol from wood fires 1: measurement and  
22 simulation of organic aerosol evolution, *Atmos. Chem. Phys.*, 9, 1263-1277, doi:10.5194/acp-  
23 9-1263-2009, 2009.

24 Harrison, R. M., Beddows, D. C. S., Hu, L., and Yin, J.: Comparison of methods for  
25 evaluation of wood smoke and estimation of UK ambient concentrations, *Atmos. Chem.*  
26 *Phys.*, 12, 8271 – 8283, doi:10.5194/acp-12-8271-2012, 2012.

27 Hawkins, L. N., and Russell, L. M.: Oxidation of ketone groups in transported biomass  
28 burning aerosol from the 2008 Northern California Lightning Series fires, *Atmos. Environ.*,  
29 44, 4142-4154, doi:10.1016/j.atmosenv.2010.07.036, 2010.

Deleted: .

1 Hennigan, C. J., Sullivan, A. P., Collett Jr., J. L., and Robinson, A. L.: Levoglucosan stability  
2 in biomass burning particles exposed to hydroxyl radicals, *Geophys. Res. Lett.*, 37, L09806,  
3 doi:10.1029/2010GL043088, 2010.

4 Herich, H., Gianini, M. F. D., Piot, C., Mocnik, G., Jaffrezo, J. L., Besombes, J. L., Prévôt, A.  
5 S. H., and Hueglin, C.: Overview of the impact of wood burning emissions on carbonaceous  
6 aerosols and PM in large parts of the Alpine region, *Atmos. Environ.*, 89, 64–75,  
7 doi:10.1016/j.atmosenv.2014.02.008, 2014

8 [Heringa, M. F., DeCarlo, P. F., Chirico, R., Tritscher, T., Dommen, J., Weingartner, E.,  
9 Richter, R., Wehrle, G., Prévôt, A. S. H., and Baltensperger, U.: Investigations of primary and  
10 secondary particulate matter of different wood combustion appliances with a high-resolution  
11 time-of-flight aerosol mass spectrometer, \*Atmos. Chem. Phys.\*, 11, 5945–5957,  
12 doi:10.5194/acp-11-5945-2011, 2011.](#)

13 Hildebrandt, L., Kostenidou, E., Lanz, V. A., Prévôt, A. S. H., Baltensperger, U.,  
14 Mihalopoulos, N., Laaksonen, A., Donahue, N. M., and Pandis, S. N.: Sources and  
15 atmospheric processing of organic aerosol in the Mediterranean: insights from aerosol mass  
16 spectrometer factor analysis, *Atmos. Chem. Phys.*, 11, 12499–12515, doi:10,5194/acp-11-  
17 12499-2011, 2011.

18 Hoffmann, D., Tilgner, A., Iinuma, Y., and Herrmann, H.: Atmospheric stability of  
19 levoglucosan: a detailed laboratory and modeling study, *Environ. Sci. Technol.*, 44, 694–699,  
20 doi:10.1021/es902476f, 2010.

21 Honrath, R., Owen, R. C., Val Martin, M., Reid, J., Lapina, K., Fialho, P., Dziobak, M.,  
22 Kleissl, J., and Westphal, D.: Regional and hemispheric impacts of anthropogenic and  
23 biomass burning emissions on summertime CO and O<sub>3</sub> in the North Atlantic lower free  
24 troposphere, *J. Geophys. Res.*, 109, doi:10.1029/2004JD005147, 2004.

25 Huang, R.-J., Zhang, Y., Bozzetti, C., Ho, K.-F., Cao, J.-J., Han, Y., Daellenbach, K. R.,  
26 Slowik, J. G., Platt, S. M., Canonaco, F., Zotter, P., Wolf, R., Pieber, S. M., Bruns, E. A.,  
27 Crippa, M., Ciarelli, G., Piazzalunga, A., Schwikowski, M., Abbaszade, G., Schnelle-Kreis,  
28 J., Zimmermann, R., An, Z., Szidat, S., Baltensperger, U., El Haddad, I., and Prévôt, A. S. H.:  
29 High secondary aerosol contribution to particulate pollution during haze events in China,  
30 *Nature*, 514(7521), 218–222, doi:10.1038/nature13774, 2014.

**Deleted:** Heringa, M. F., P. F. DeCarlo, R. Chirico, T. Tritscher, J. Dommen, E. Weingartner, R. Richter, G. Wehrle, A. S. H. Prévôt, and Baltensperger U.: Investigations of primary and secondary particulate matter of different wood combustion appliances with a high-resolution time-of-flight aerosol mass spectrometer, *Atmos. Chem. Phys.*, 11(12), 5945–5957, 2011

1 Jimenez, J. L., Canagaratna, M. R., Donahue, N. M., Prévôt, A. S. H., Zhang, Q., Kroll, J. H.,  
2 DeCarlo, P. F., Allan, J. D., Coe, H., Ng, N. L., Aiken, A. C., Docherty, K. S., Ulbrich, I. M.,  
3 Grieshop, A. P., Robinson, A. L., Duplissy, J., Smith, J. D., Wilson, K. R., Lanz, V. A.,  
4 Hueglin, C., Sun, Y. L., Tian, J., Laaksonen, A., Raatikainen, T., Rautiainen, J., Vaattovaara,  
5 P., Ehn, M., Kulmala, M., Tomlinson, J. M., Collins, D. R., Cubison, M. J., Dunlea, E. J.,  
6 Huffman, J. A., Onasch, T. B., Alfarra, M. R., Williams, P. I., Bower, K., Kondo, Y.,  
7 Schneider, J., Drewnick, F., Borrmann, S., Weimer, S., Demerjian, K., Salcedo, D., Cottrell,  
8 L., Griffin, R., Takami, A., Miyoshi, T., Hatakeyama, S., Shimono, A., Sun, J. Y., Zhang, Y.  
9 M., Dzepina, K., Kimmel, J. R., Sueper, D., Jayne, J. T., Herndon, S. C., Trimborn, A. M.,  
10 Williams, L. R., Wood, E. C., Middlebrook, A. M., Kolb, C. E., Baltensperger, U., and  
11 Worsnop, D. R.: Evolution of organic aerosols in the atmosphere, *Science*, 326, 1525 - 1529,  
12 doi:10.1126/science.1180353, 2009.

13 Kanamitsu, M., Ebisuzaki, W., Woollen, J., Yang, S. K., Hnilo, J. J., Fiorino, M., and Potter,  
14 G. L.: NCEP-DOE AMIP-II reanalysis (R-2), *Bull. Am. Meteorol. Soc.*, 83, 1631–1643,  
15 doi:10.1175/BAMS-83-11-1631, 2002.

16 Kikas, U., Reinart, A., Pugatshova, A., Tamm, E., and Ulevicius, V.: Microphysical, chemical  
17 and optical aerosol properties in the Baltic Sea region, *Atmos. Res.*, 90(2–4), 211–222,  
18 doi:10.1016/j.atmosres.2008.02.009, 2008.

19 Lanz, V. A., Alfarra, M. R., Baltensperger, U., Buchmann, B., Hueglin, C., and Prévôt, A. S.  
20 H.: Source apportionment of submicron organic aerosols at an urban site by linear unmixing  
21 of aerosol mass spectra, *Atmos. Chem. Phys.*, 7, 1503-1522, 2007.

22 Lanz, V. A., Prévôt, A. S. H., Alfarra, M. R., Weimer, S., Mohr, C., DeCarlo, P. F., Gianini,  
23 M. F. D., Hueglin, C., Schneider, J., Favez, O., D'Anna, B., George, C., and Baltensperger,  
24 U.: Characterization of aerosol chemical composition with aerosol mass spectrometry in  
25 Central Europe: an overview, *Atmos. Chem. Phys.*, 10, 10453–10471, doi:10.5194/acp-10-  
26 10453-2010, 2010.

27 Lavanchy, V. M. H., Gäggeler, H. W., Schotterer, U., Schwikowski, M., and Baltensperger,  
28 U.: Historical record of carbonaceous particle concentrations from a European high-alpine  
29 glacier (Colle Gnifetti, Switzerland), *J. Geophys. Res. Atmos.*, 104, 21227–21236,  
30 doi:10.1029/1999jd900408, 1999.

Deleted: M. R.

Deleted: U.

Deleted: B.

Deleted: C.

Deleted: A. S. H.

1 Lemire, K. R., Allen, D. T., Klouda, G. A., and Lewis, C. W.: Fine particulate matter source  
2 attribution for southeast Texas using  $^{14}\text{C}/^{13}\text{C}$  ratios, *J. Geophys. Res.*, 107(D22), 4613,  
3 doi:10.1029/2002JD002339, 2002.

4 Levine, J. S. 1996. *Biomass Burning And Global Change*, Cambridge, MA, MIT Press.

5 Lewis, C. W., Klouda, G. A., and Ellenson, W. D.: Radiocarbon measurement of the biogenic  
6 contribution to summertime PM-2.5 ambient aerosol in Nashville, TN, *Atmos. Environ.*, 38,  
7 6053–6061, doi:10.1016/j.atmosenv.2004.06.011, 2004.

8 Mann, G. W., Carslaw, K. S., Reddington, C. L., Pringle, K. J., Schulz, M., Asmi, A.,  
9 Spracklen, D. V., Ridley, D. A., Woodhouse, M. T., Lee, L. A., Zhang, K., Ghan, S. J., Easter,  
10 R. C., Liu, X., Stier, P., Lee, Y. H., Adams, P. J., Tost, H., Lelieveld, J., Bauer, S. E.,  
11 Tsigaridis, K., van Noije, T. P. C., Strunk, A., Vignati, E., Bellouin, N., Dalvi, M., Johnson,  
12 C. E., Bergman, T., Kokkola, H., von Salzen, K., Yu, F., Luo, G., Petzold, A., Heintzenberg,  
13 J., Clarke, A., Ogren, J. A., Gras, J., Baltensperger, U., Kaminski, U., Jennings, S. G.,  
14 O'Dowd, C. D., Harrison, R. M., Beddows, D. C. S., Kulmala, M., Viisanen, Y., Ulevicius, V.,  
15 Mihalopoulos, N., Zdimal, V., Fiebig, M., Hansson, H.-C., Swietlicki, E., and Henzing, J. S.:  
16 Intercomparison and evaluation of global aerosol microphysical properties among AeroCom  
17 models of a range of complexity, *Atmos. Chem. Phys.*, 14, 4679-4713, doi:10.5194/acp-14-  
18 4679-2014, 2014.

19 Masalaite, A., Remeikis, V., Garbaras, A., Dudoitis, V., Ulevicius, V., and Ceburnis, D.:  
20 Elucidating carbonaceous aerosol sources by the stable carbon  $\delta^{13}\text{C}$  TC ratio in size-  
21 segregated particles, *Atmos. Res.*, 158–159, 1-12, doi:10.1016/j.atmosres.2015.01.014, 2015.

22 Matthew, B. M., Middlebrook, A. M., and Onasch, T. B.: Collection efficiencies in an  
23 Aerodyne aerosol mass spectrometer as a function of particle phase for laboratory generated  
24 aerosols, *Aerosol Sci. Tech.*, 42, 884–898, doi:10.1080/02786820802356797, 2008.

25 Middlebrook, A. M., Bahreini, R., Jimenez, J. L., and Canagaratna, M. R.: Evaluation of  
26 composition-dependent collection efficiencies for the Aerodyne aerosol mass spectrometer  
27 using field data, *Aerosol Sci. Technol.*, 46, 258-271, doi:10.1080/02786826.2011.620041,  
28 2012.

29 Minguillón, M. C., Perron, N., Querol, X., Szidat, S., Fahrni, S. M., Alastuey, A., Jimenez, J.  
30 L., Mohr, C., Ortega, A. M., Day, D. A., Lanz, V. A., Wacker, L., Reche, C., Cusack, M.,  
31 Amato, F., Kiss, G., Hoffer, A., Decesari, S., Moretti, F., Hillamo, R., Teinilä, K., Seco, R.,

1 Peñuelas, J., Metzger, A., Schallhart, S., Müller, M., Hansel, A., Burkhardt, J. F.,  
2 Baltensperger, U., and Prévôt, A. S. H.: Fossil versus contemporary sources of fine elemental  
3 and organic carbonaceous particulate matter during the DAURE campaign in Northeast Spain,  
4 *Atmos. Chem. Phys.*, 11, 12067-12084, doi:10.5194/acp-11-12067-2011, 2011.

5 Mochida, M., Kawamura, K., Fu, P. Q., and Takemura, T.: Seasonal variation of levoglucosan  
6 in aerosols over the western North Pacific and its assessment as a biomass-burning tracer,  
7 *Atmos. Environ.*, 44, 3511–3518, doi:10.1016/j.atmosenv.2010.06.017, 2010.

8 MODIS NASA LANCE - FIRMS, 2011, MODIS Active Fire Detections, Data set, Available  
9 on – line: <http://earthdata.nasa.gov/data/nrt-data/firms>.

10 Mohr, C., Huffman, J. A., Cubison, M. J., Aiken, A. C., Docherty, K. S., Kimmel, J. R.,  
11 Ulbrich, I. M., Hannigan, M., and Jimenez, J. L.: Characterization of Primary Organic  
12 Aerosol 25 Emissions from Meat Cooking, Trash Burning, and Motor Vehicles with High-  
13 Resolution Aerosol Mass Spectrometry and Comparison with Ambient and Chamber  
14 Observations, *Environ. Sci. Technol.*, 43, 2443–2449, doi:10.1021/es8011518, 2009.

15 Mordas, G., Ulevicius, V., Plauškaitė, K., and Prokopčiuk, N.: Validation of the condensation  
16 particle counter UF-02M in laboratory and ambient conditions, *Lith. J. Phys.*, 53 (3), 175-182,  
17 2013.

18 Ng, N. L., Herndon, S. C., Trimborn, A., Canagaratna, M. R., Croteau, P. L., Onasch, T. B.  
19 Sueper, D., Worsnop, D. R., Zhang, Q., Sun, Y. L., and Jayne, J. T.: An Aerosol Chemical  
20 Speciation Monitor (ACSM) for routine monitoring of the composition and mass  
21 concentrations of ambient aerosol, *Aerosol Sci. Tech.*, 45, 770-784,  
22 doi:10.1080/02786826.2011.560211, 2011.

23 Oanh, N. T. K., Ly, B. T., Tipayarom, D., Manandhar, B. R., Prapat, P., Simpson, C. D., and  
24 Liu, L. J. S.: Characterization of particulate matter emission from open burning of rice straw,  
25 *Atmos. Environ.*, 45, 493 - 502, doi:10.1016/j.atmosenv.2010.09.023 2011.

26 Orasche, J., Schnelle-Kreis, J., Abbaszade, G., and Zimmermann, R.: Technical Note: In-situ  
27 derivatization thermal desorption GC-TOFMS for direct analysis of particle-bound non-polar  
28 and polar organic species, *Atmos. Chem. Phys.*, 11, 8977-8993, doi:10.5194/acp-11-8977-  
29 2011, 2011.

1 Orasche, J., Seidel, T., Hartmann, H., Schnelle-Kreis, J., Chow, J.C, Ruppert, H., and  
2 Zimmermann R.: Comparison of emissions from wood combustion. Part 1: Emission factors  
3 and characteristics from different small-scale residential heating appliances considering  
4 particulate matter and polycyclic aromatic hydrocarbon (PAH)-related toxicological potential  
5 of particle-bound organic species, *Energy Fuels*, 26(11), 6695-6704, doi: 10.1021/ef301295k,  
6 2012.

7 Oros, D. R., Radzi bin Abas, M., Omar, N. Y. M. J., Rahman, N. A., and Simoneit, B. R. T.:  
8 Identification and emission factors of molecular tracers in organic aerosols from biomass  
9 burning: 3. Grasses, *Appl. Geochem.*, 21, 919–940, doi:10.1016/j.apgeochem.2006.01.008  
10 2006.

11 Paatero, P.: Least squares formulation of robust non-negative factor analysis, *Chemometr.  
12 Intell. Lab.*, 37, 23–35, doi:10.1016/S0169-7439(96)00044-5, 1997.

13 Paatero, P. and Tapper, U.: Positive matrix factorization – a nonnegative factor model with  
14 optimal utilization of error-estimates of data values, *Environmetrics*, 5, 111–126,  
15 doi:10.1002/env.3170050203, 1994.

16 Paatero, P., Eberly, S., Brown, S. G., and Norris, G. A.: Methods for estimating uncertainty in  
17 factor analytic solutions, *Atmos. Meas. Tech.*, 7, 781-797, doi:10.5194/amt-7-781-2014,  
18 2014.

19 Popovicheva, O., Kistler, M., Kireeva, E., Persiantseva, N., Timofeev, M., Kopeikin, V., and  
20 Kasper-Giebl, A.: Physicochemical characterization of smoke aerosol during large-scale  
21 wildfires: extreme event of August 2010 in Moscow, *Atmos. Environ.*, 96: 405–414,  
22 doi:10.1016/j.atmosenv.2014.03.026, 2014.

23 Puxbaum, H., Caseiro, A., Sánchez-Ochoa, A., Kasper-Giebl, A., Claeys, M., Gelencsér, A.,  
24 Legrand, M., Preunkert, S., and Pio, C.: Levoglucosan levels at background sites in Europe  
25 for assessing the impact of biomass combustion on the European aerosol background, *J.  
26 Geophys. Res.*, 112 (D23S05), doi:10.1029/2006JD008114, 2007.

27 Reid, J. S., Prins, E. M., Westphal, D. L., Schmidt, C. C., Richardson, K. A., Christopher, S.  
28 A., Eck, T. F., Reid, E. A., Curtis, C. A., and Hoffman, J. P.: Real-time monitoring of South  
29 American smoke particle emissions and transport using a coupled remote sensing/box-model  
30 approach, *Geophys. Res. Lett.*, 31, L06107, doi:10.1029/2003GL018845, 2004.

1 Rutter, A. P., Snyder, D. C., Schauer, J. J., DeMinter, J., and Shelton, B.: Sensitivity and bias  
2 of molecular marker-based aerosol source apportionment models to small contributions of  
3 coal combustion soot. *Environ. Sci. Technol.* 43, 7770-7777, 2009.

4 Saarikoski, S., Sillanpaa, M., Sofiev, M., Timonen, H., Saarnio, K., Teinela, K., Karppinen,  
5 A., Kukkonen, J., and Hillamo, R.: Chemical composition of aerosols during a major biomass  
6 burning episode over northern Europe in spring 2006: Experimental and modelling  
7 assessments, *Atmos. Environ.*, 41, 3577–3589, doi:10.1016/j.atmosenv.2006.12.053, 2007.

8 Salazar, G., Zhang, Y. L., Agrios, K., and Szidat, S.: Development of a method for fast and  
9 automatic radiocarbon measurement of aerosol samples by online coupling of an elemental  
10 analyzer with a MICADAS AMS, *Nucl. Instrum. Meth. Phys. Res. B.*, 361, 163-167,  
11 doi:10.1016/j.nimb.2015.03.051, 2015.

12 Schmidl, C., Marr, I. L., Caseiro, A., Kotianová, P., Berner, A., Bauer, H., Kasper-Giebl, A.,  
13 and Puxbaum, H.: Chemical characterisation of fine particle emissions from wood stove  
14 combustion of common woods growing in mid-European Alpine regions, *Atmos. Environ.*,  
15 42(1), 126-141, 2008.

16 Sofiev, M., Siljamo, P., Valkama, I., Ilvonen, M., and Kukkonen, J.: A dispersion modelling  
17 system SILAM and its evaluation against ETEX data, *Atm. Env.*, 40, 674–685,  
18 doi:10.1016/j.atmosenv.2005.09.069, 2006.

19 Stein, A. F., Draxler, R. R., Rolph, G. D., Stunder, B. J. B., Cohen, M. D., and Ngan, F.:  
20 NOAA's HYSPLIT atmospheric transport and dispersion modeling system, *Bull. Amer.*  
21 *Meteor. Soc.*, 96, 2059–2077, 2015.

22 Sullivan, A. P., Holden, A. S., Patterson, L. A., McMeeking, G. R., Kreidenweis, S. M.,  
23 Malm, W. C., Hao, W. M., Wold, C. E., and Collett Jr. J. L.: A method for smoke marker  
24 measurements and its potential application for determining the contribution of biomass  
25 burning from wildfires and prescribed fires to ambient PM<sub>2.5</sub> organic carbon, *J. Geophys.*  
26 *Res.*, 113, D22302, doi:10.1029/2008JD010216, 2008.

27 [Sullivan, A. P., May, A. A., Lee, T., McMeeking, G. R., Kreidenweis, S. M., Akagi, S. K.,  
28 Yokelson, R. J., Urbanski, S. P., and Collett Jr., J. L.: Airborne characterization of smoke  
29 marker ratios from prescribed burning, \*Atmos. Chem. Phys.\*, 14, 10535-10545,  
30 doi:10.5194/acp-14-10535-2014, 2014.](#)

Deleted:

Deleted: Sullivan, A. P., A. A. May, T. Lee, G. R. McMeeking, S. M. Kreidenweis, S. K. Akagi, R. J. Yokelson, S. P. Urbanski and J. L. Collett, Jr.: Airborne characterization of smoke marker ratios from prescribed burning, *Atm. Chem. Phys.* 14(19): 10535-10545, 2014

1 Sun, Y. L., Wang, Z. F., Dong, H. B., Yang, T., Li, J., Pan, X. L., Chen, P., and Jayne, J. T.:  
2 Characterization of summer organic and inorganic aerosols in Beijing, China with an aerosol  
3 chemical speciation monitor, *Atmos. Environ.*, 51, 250–259,  
4 doi:10.1016/j.atmosenv.2012.01.013, 2012.

5 Szidat, S., Jenk, T. M., Gäggeler, H. W., Synal, H.-A., Fisseha, R., Baltensperger, U.,  
6 Kalberer, M., Samburova, V., Reimann, S., Kasper-Giebl, A., and Hajdas, I.: Radiocarbon  
7 (<sup>14</sup>C)-deduced biogenic and anthropogenic contributions to organic carbon (OC) of urban  
8 aerosols from Zurich, Switzerland, *Atmos. Environ.*, 38, 4035–4044,  
9 doi:10.1016/j.atmosenv.2004.03.066, 2004.

10 Szidat, S., Salazar, G. A., Vogel, E., Battaglia, M., Wacker, L., Synal, H.-A., and Türlér, A.:  
11 <sup>14</sup>C analysis and sample preparation at the new Bern Laboratory for the analysis of  
12 radiocarbon with AMS (LARA), *Radiocarbon*, 56, 561–566, doi:10.2458/56.17457, 2014.

13 Timonen, H., Aurela, M., Carbone, S., Saarnio, K., Saarikoski, S., Mäkelä, T., Kulmala, M.,  
14 Kerminen, V.-M., Worsnop, D. R., and Hillamo, R.: High time-resolution chemical  
15 characterization of the water soluble fraction of ambient aerosols with PILS-TOC-IC and  
16 AMS. *Atmos. Meas. Tech.* 3:1063–1074, doi:10.5194/amt-3-1063-2010, 2010.

17 Turekian, V. C., Macko, S., Ballentine, D., Swap, R. J., and Garstang, M.: Causes of bulk  
18 carbon and nitrogen isotopic fractionations in the products of vegetation burns: laboratory  
19 studies, *Chem. Geol.*, 152, 181–192, doi:10.1016/S0009-2541(98)00105-3 1998.

20 Ulbrich, I. M., Canagaratna, M. R., Zhang, Q., Worsnop, D. R., and Jimenez, J. L.:  
21 Interpretation of organic components from Positive Matrix Factorization of aerosol mass  
22 spectrometric data, *Atmos. Chem. Phys.*, 9, 2891–2918, doi:10.5194/acp-9-2891-2009, 2009.

23 Ulevicius, V., Byčėnkiėnė, S., Remeikis, V., Garbaras, A., Kecorius, S., Andriejauskienė, J.,  
24 Jasinevičienė, D., and Močnik, G.: Characterization of aerosol particle episodes in Lithuania  
25 caused by long-range and regional transport, *Atmos. Res.*, 98(2–4), 190–200,  
26 doi:10.1016/j.atmosres.2010.03.02, 2010a.

27 Ulevicius, V., Byčėnkiėnė, S., Špirkauskaitė, N., and Kecorius, S.: Biomass burning impact  
28 on black carbon aerosol mass concentration at a coastal site: case studies, *Lith. J. Phys.*, 50(3),  
29 335–344, doi:10.3952/lithjphys.50304, 2010b.

1 Widory, D.: Nitrogen isotopes: Tracers of origin and processes affecting PM<sub>10</sub> in the  
2 atmosphere of Paris, *Atmos. Environ.*, 41, 2382-2390, doi:10.1016/j.atmosenv.2006.11.009,  
3 2007.

4 Weimer, S., Alfara, M.R., Schreiber, D., Mohr, M., Prévôt, A.S.H., and Baltensperger U.:  
5 Organic aerosol mass spectral signatures from wood burning emissions: Influence of burning  
6 conditions and wood type, *J. Geophys. Res.*, 113, D10304, doi:10.1029/2007JD009309, 2008.

7 Wiedensohler, A., Birmili, W., Nowak, A., Sonntag, A., Weinhold, K., Merkel, M., Wehner,  
8 B., Tuch, T., Pfeifer, S., Fiebig, M., Fjåraa, A. M., Asmi, E., Sellegri, K., Depuy, R., Venzac,  
9 H., Villani, P., Laj, P., Aalto, P., Ogren, J. A., Swietlicki, E., Williams, P., Roldin, P.,  
10 Quincey, P., Hüglin, C., Fierz-Schmidhauser, R., Gysel, M., Weingartner, E., Riccobono, F.,  
11 Santos, S., Grünig, C., Faloon, K., Beddows, D., Harrison, R., Monahan, C., Jennings, S. G.,  
12 O'Dowd, C. D., Marinoni, A., Horn, H.-G., Keck, L., Jiang, J., Scheckman, J., McMurry, P.  
13 H., Deng, Z., Zhao, C. S., Moerman, M., Henzing, B., de Leeuw, G., Löschau, G., and  
14 Bastian S.: Mobility particle size spectrometers: harmonization of technical standards and  
15 data structure to facilitate high quality long-term observations of atmospheric particle number  
16 size distributions. *Atmos. Meas. Tech.*, 5, 657–685. doi:10.5194/amt-5-657-2012, 2012.

17 Yttri, K. E., Simpson, D., Nøjgaard, J. K., Kristensen, K., Genberg, J., Stenström, K.,  
18 Swietlicki, E., Hillamo, R., Aurela, M., Bauer, H., Offenberg, J. H., Jaoui, M., Dye, C.,  
19 Eckhardt, S., Burkhardt, J. F., Stohl, A., and Glasius, M.: Source apportionment of the summer  
20 time carbonaceous aerosol at Nordic rural background sites, *Atmos., Chem. Phys.*, 11, 13339-  
21 13357, doi:10.5194/acp-11-13339-2011, 2011.

22 Yttri, K. E., Lund Myhre, C., Eckhardt, S., Fiebig, M., Dye, C., Hirdman, D., Ström, J.,  
23 Klimont, Z., and Stohl, A.: Quantifying black carbon from biomass burning by means of  
24 levoglucosan – a one-year time series at the Arctic observatory Zeppelin, *Atmos. Chem.*  
25 *Phys.*, 14, 6427-6442, doi:10.5194/acp-14-6427-2014, 2014.

26 Zawadzka, O., Makuch, P., Krzysztof, M., Markowicz., Zieliński, T., Petelski, T., Ulevicius,  
27 V., Strzałkowska, A., Rozwadowska, A., and Gutowska, D.: Studies of aerosol optical depth  
28 with the use of microtops II sun photometers and MODIS detectors in coastal areas of the  
29 Baltic Sea, *Acta Geophys.*, 62 (2), 400-422, doi:10.2478/s11600-013-0182-5, 2013.

30 Zhang, Y. L., Perron, N., Ciobanu, V. G., Zotter, P., Minguillon, M. C., Wacker, L., Prévôt,  
31 A. S. H., Baltensperger, U., and Szidat, S.: On the isolation of OC and EC and the optimal

1 strategy of radiocarbon based source apportionment of carbonaceous aerosols, *Atmos. Chem.*  
2 *Phys.*, 12 (22), 10841–10856, doi:10.5194/acp-12-10841-2012, 2012.

3 Zhang, Y.-L., Huang, R.-J., El Haddad, I., Ho, K.-F., Cao, J.-J., Han, Y., Zotter, P., Bozzetti,  
4 C., Daellenbach, K. R., Canonaco, F., Slowik, J. G., Salazar, G., Schwikowski, M., Schnelle-  
5 Kreis, J., Abbaszade, G., Zimmermann, R., Baltensperger, U., Prévôt, A. S. H., and Szidat, S.:  
6 Fossil vs. non-fossil sources of fine carbonaceous aerosols in four Chinese cities during the  
7 extreme winter haze episode of 2013, *Atmos. Chem. Phys.*, 15, 1299-1312, doi:10.5194/acp-  
8 15-1299-2015, 2015.

9 Zotter, P., Ciobanu, V. G., Zhang, Y. L., El-Haddad, I., Macchia, M., Daellenbach, K. R.,  
10 Salazar, G. A., Huang, R. J., Wacker, L., Hueglin, C., Piazzalunga, A., Fermo, P.,  
11 Schwikowski, M., Baltensperger, U., Szidat, S., and Prevot A. S. H.: Radiocarbon analysis of  
12 elemental and organic carbon in Switzerland during winter-smog episodes from 2008 to 2012-  
13 Part 1: Source apportionment and spatial variability, *Atmos. Chem. Phys.*, 14(24), 13551-  
14 13570, 2014.

15

16

The Baltic Sea Area



1  
2  
3  
4  
5  
6

Figure 1. A) Map of the observation site, Preila (indicated by the red mark). Nearest major cities are Klaipeda (40 km north) and Kaliningrad (90 km south), B) Environmental pollution research station Preila and site surroundings (C).

1 Table 1. Preila site surroundings 10 km

Site altitude	5 (m) a.s.l.	Terrain below site <sup>1</sup>	50.0 (%)
Median altitude	0 (m) a.s.l.	Standard deviation of altitude <sup>2</sup>	7 (m)
Total population	6831	Standard deviation of population	159
Mean population density <sup>3</sup>	20 (km <sup>-2</sup> )	Standard deviation of population density	13 (km <sup>-2</sup> )
Local population density	29.5 (km <sup>-2</sup> )		
Dominating land cover types (based on GLC2000)			
Water bodies (natural & artificial) (20 <sup>*</sup> )			84.9 (%)
Tree cover, needle-leaved, evergreen (4 <sup>*</sup> )			13.2 (%)
Tree cover, mixed leaf type (6 <sup>*</sup> )			1.1 (%)
Herbaceous cover, closed-open (13 <sup>*</sup> )			0.4 (%)

2 [\\* GLC2000 classes ID](#)

3

<sup>1</sup>Percentage of terrain within 10 km radius from the site that lies at lower altitudes than the site itself based on GLOBE 30" (arc-seconds) topography data. For an elevated site this percentage will be large (close to 100%), while for sites within valleys or basins this percentage will be small. For sites within homogeneous terrain the percentage will be 50%. Such sites can be assumed to be more representative for a larger area, while for sites in more complex terrain small circulation systems might influence the surface concentration field and introduce large heterogeneities.

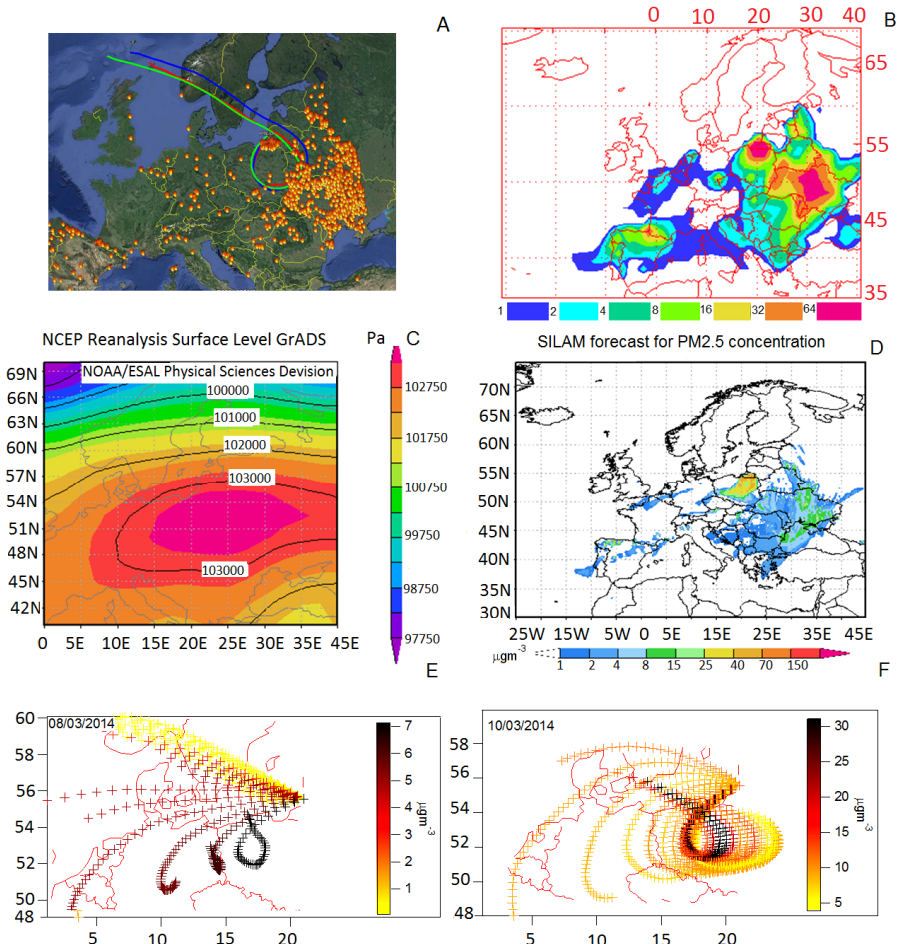
<sup>2</sup> Standard deviation of population density within a 10 km radius from the site based on GPW3 2.5' (arc-minutes) population data. Large variations within the population density pattern around a site might introduce large differences in the pollutant levels depending on wind direction. Measurements at sites with small standard deviation of population density in the surroundings are therefore thought to be more representative of a larger domain and the mean population density.

<sup>3</sup> [Mean population density within a 10 km radius from the site based on GPW3 2.5' \(arc-minutes\) population data. Small population densities are usually connected with little emissions. Measurements at sites with small population density in the surroundings are therefore thought to be more representative of a larger domain.](#)

Deleted: <sup>4</sup>

Deleted:

Deleted:



1  
 2  
 3 Figure 2. (A) Combined MODIS images observed from the Aqua satellite on 10 March 2014,  
 4 showing numerous fires due to seasonal grass burning and 72-hour air mass backward  
 5 trajectories from the fire regions arriving at Preila at 100 (red), 200 (blue) and 500 (green) m  
 6 above ground level (AGL). (B) NAAPS model results showing surface smoke concentrations  
 7 for the strongest stage (10 March 2014) (the color scale (from blue to purple) corresponds to  
 8 the 7 levels of the contours that indicate the smoke mass mixing ratio ( $\mu\text{g m}^{-3}$ ) at the surface).  
 9 Smoke optical depth at a wavelength of 0.55 microns. The contouring begins at 1  $\mu\text{g m}^{-3}$  and

1 doubles in magnitude for each successive contour. (C) Pressure level in Pa at the surface for  
2 2.5 degree latitude  $\times$  2.5 degree longitude global grids (NCEP/NCAR Reanalysis 1, 10 March  
3 2014). (D) PM<sub>2.5</sub> concentration ( $\mu\text{g m}^{-3}$ ) forecast utilized by the SILAM chemical transport  
4 model during the event of grass fires. (E, F) ACSM organics concentration ( $\mu\text{g m}^{-3}$ )  
5 (measured in Preila) weighted air mass back trajectories of 48 h (for an arrival on 8 (E) and 10  
6 (F) March 2014) with an altitude endpoint of 500 m AGL.

7

8

9

10

11

12

13

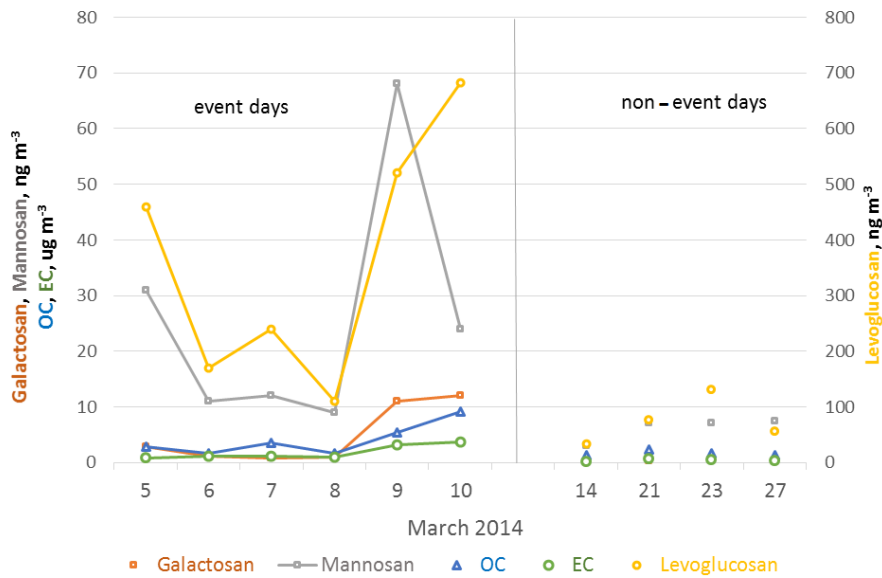
14

15

16

17

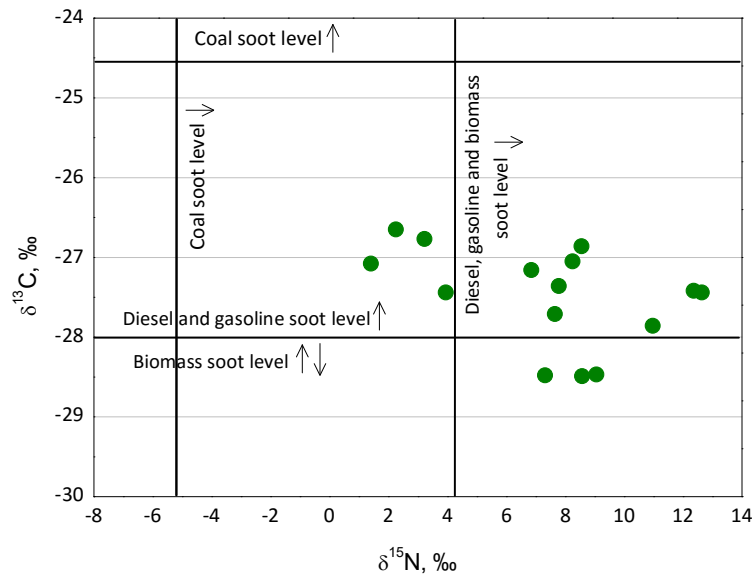
18



1  
 2 Figure 3. Average daily concentration during event days (from 5 to 10 March 2014) and non-  
 3 event days (14, 21, 23 and 27 March 2014) for levoglucosan, galactosan, mannosan (in ng m<sup>-3</sup>)  
 4 and for elemental carbon (EC) and organic carbon (OC) in μg m<sup>-3</sup>.

5  
 6

1



2

3 Figure 4. Stable carbon and nitrogen isotope ratio values of PM<sub>1</sub> in Preila station. Vertical and  
4 horizontal lines represent carbon and nitrogen, respectively, isotope ratio characteristic values  
5 for the sources of aerosol particles (Garbaras et al., 2008, 2015; Ulevicius et al., 2010a;  
6 Widory 2007).

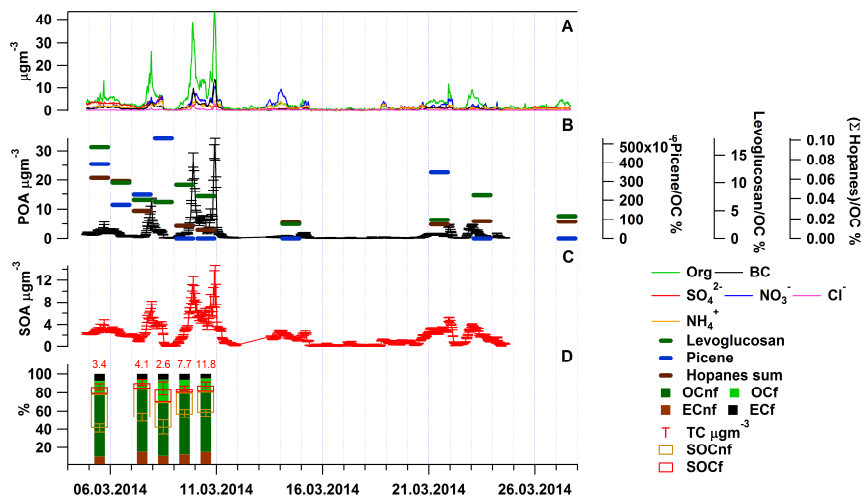
7

1 Table 2. Variation of the fractions of EC<sub>f</sub>, EC<sub>nf</sub>, OC<sub>f</sub>, OC<sub>nf</sub> and TC, EC and OC values during  
 2 the study periods.

Date of collection	EC <sub>f</sub> μg m <sup>-3</sup>	EC <sub>nf</sub> μg m <sup>-3</sup>	OC <sub>f</sub> μg m <sup>-3</sup>	OC <sub>nf</sub> μg m <sup>-3</sup>	TC μg m <sup>-3</sup>	EC μg m <sup>-3</sup>	OC μg m <sup>-3</sup>
2014.03.05	0.25±0.04	0.33	0.47±0.10	2.34±0.18	3.39±0.18	0.59±0.17	2.80±0.18
2014.03.07	0.21±0.04	0.61	0.39±0.12	2.80±0.20	4.01±0.23	0.81±0.24	3.31±0.20
2014.03.08	0.15±0.05	0.26	0.56±0.07	1.46±0.12	2.43±0.13	0.41±0.18	2.24±0.15
2014.03.09	0.46±0.16	0.95	0.95±0.18	4.98±0.36	7.28±0.43	1.36±0.63	6.32±0.35
2014.03.10	0.56±0.18	1.64	1.64±0.28	7.77±0.50	11.72±0.64	2.31±0.75	9.47±0.51

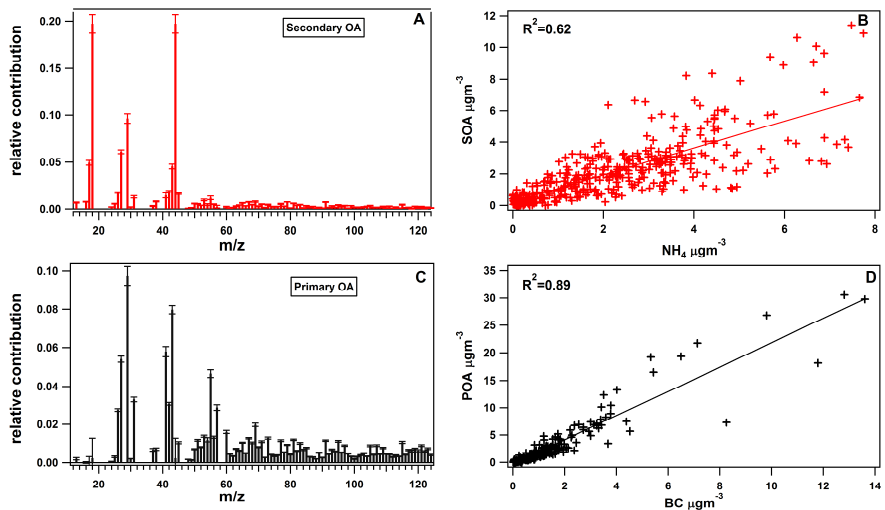
3

4



1  
 2 Figure 5. Average chemical composition and time series of NR-PM<sub>1</sub> OA for the entire study  
 3 (A), B) Time series of the POA factor and percent contribution of the corresponding tracer  
 4 species (levoglucosan, picene and hopanes) to total OA, C) Time series of the SOA factor, D)  
 5 Relative source apportionment of TC during the BB event. Numbers indicate the total carbon  
 6 absolute concentrations in  $\mu\text{g m}^{-3}$ , variations of the mass concentrations of the SOC<sub>f</sub> and  
 7 SOC<sub>nf</sub> (the whiskers above and below the boxes indicate the 1<sup>st</sup> and 3<sup>rd</sup> quartiles).

8  
 9  
 10  
 11  
 12  
 13  
 14  
 15

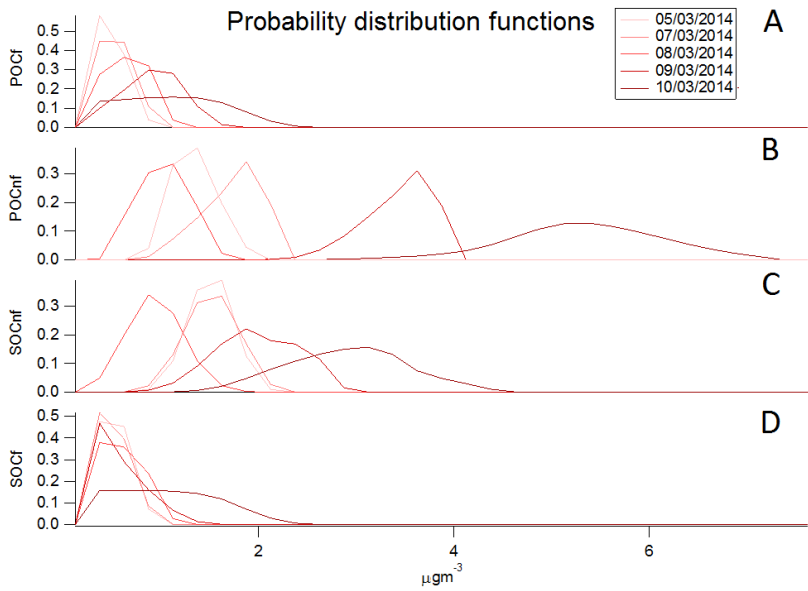


1  
 2 Figure 6. Mass spectra of SOA and POA, error bars represent the standard deviation of 20  
 3 PMF runs (A,C) and the scatter plots illustrate the relationship between SOA and  $\text{NH}_4^+$  (B)  
 4 and POA with BC (D).  
 5

1 Table 3. Average percentage contributions of different sources

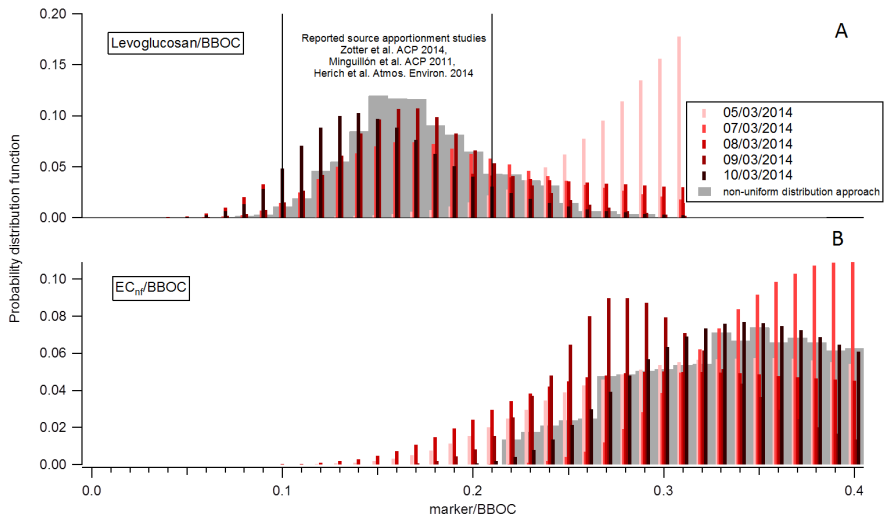
<u>Relative contributions [%] to TC</u>	<u>POCf</u>	<u>POCnf</u>	<u>SOCf</u>	<u>SOCnf</u>	<u>ECf</u>	<u>ECnf</u>	<u>TC to PM1</u>
<u>2014.03.05</u>	<u>5.1</u>	<u>43.2</u>	<u>6.7</u>	<u>22.5</u>	<u>9.7</u>	<u>12.8</u>	<u>28.4</u>
<u>2014.03.07</u>	<u>6.2</u>	<u>43.6</u>	<u>5.7</u>	<u>19.1</u>	<u>6.6</u>	<u>18.8</u>	<u>37.6</u>
<u>2014.03.08</u>	<u>7.7</u>	<u>26.3</u>	<u>13.4</u>	<u>18.6</u>	<u>12.6</u>	<u>21.4</u>	<u>24.8</u>
<u>2014.03.09</u>	<u>4.5</u>	<u>41.3</u>	<u>4.4</u>	<u>13.1</u>	<u>12.5</u>	<u>24.2</u>	<u>51.3</u>
<u>2014.03.10</u>	<u>6.8</u>	<u>43.0</u>	<u>5.9</u>	<u>14.8</u>	<u>7.2</u>	<u>22.3</u>	<u>43.9</u>
<u>Relative contributions [%] to OC</u>	<u>POCf</u>	<u>POCnf</u>	<u>SOCf</u>	<u>SOCnf</u>	-	-	-
<u>2014.03.05</u>	<u>6.6</u>	<u>55.8</u>	<u>8.6</u>	<u>29.0</u>			
<u>2014.03.07</u>	<u>8.4</u>	<u>58.4</u>	<u>7.6</u>	<u>25.6</u>			
<u>2014.03.08</u>	<u>11.7</u>	<u>39.8</u>	<u>20.2</u>	<u>28.3</u>			
<u>2014.03.09</u>	<u>7.2</u>	<u>65.2</u>	<u>6.9</u>	<u>20.7</u>			
<u>2014.03.10</u>	<u>9.6</u>	<u>61.0</u>	<u>8.4</u>	<u>21.0</u>			

2  
3  
4  
5  
6



1  
2  
3  
4  
5

Figure 7. Probability distribution functions of the absolute daily contribution of  $POC_f$  (A),  $POC_{nf}$  (B),  $SOC_{nf}$  (C),  $SOC_f$  (D).



1

2

3 Figure 8. Probability distribution functions of Levoglucosan/BBOC (A) and EC<sub>nf</sub>/BBOC (B).